Tidal asymmetry and residual sediment transport in estuaries

Z. B. Wang, C. Jeuken, H.J. de Vriend

December, 1999

Contents

Appendices

1 Introduction

1.1 Background

The Western Scheldt is one of the remaining open estuaries in The Netherlands that is strongly influenced by man. Land reclamation has reduced the size of the estuary by 40 % in less than 300 years. In this century the dredging and dumping activities have increased from less than 0.5 Mm^3/year in 1950 to over 15 Mm^3/year in 1975 (Vroon et al, 1997, Van den Berg et al, 1996). In recent years, a large dredging and dumping program has been executed to enlarge and maintain the navigation route to Antwerp. Since 1997 a deepening program is in progress and a new dredging and dumping program is initiated. For the various water management aspects, e.g. flood control and ecological functioning of the estuary, it is important to understand the impacts of human interference on the morphological development of the estuary in combination with the ever changing natural forcing, e.g. via tide, sea level rise etc.

The natural morphological development is the result of interactions between water motion, sediment transport and bed topography. In an estuary like the Western Scheldt where tidal action is an important forcing factor, it is the residual sediment transport that determines the morphological development. Therefore insight into the processes and mechanisms influencing the residual sediment transport plays a key role in the understanding of the morphological development of the estuary under the influence of changing natural conditions and human interference.

An important factor causing residual sediment transport in estuaries is tidal asymmetry. In the Western Scheldt it is possibly a principal factor influencing the sediment exchange between the ebb tidal delta and the estuary, as well as between the various parts of the estuary. Analyses of the historical data on tide and morphological development in the Western Scheldt (Gerritsen et al, 1999) indicate that there is a clear relation between the change of asymmetry of the vertical tide and the morphological development in the estuary. It is also shown that there is probably a direct relation between the asymmetry of the vertical tide and the net sediment flux. Insight into the generation of tidal asymmetry and its influence on the residual sediment transport is required for answering questions like:

- will the estuary drown under influence of sea level rise or will it silt up fast enough to keep up with the sea level?
- will there be a return flow of sediment between the dumping locations in the western part of the estuary and the dredging sites in the eastern part?
- can sand mining be continued without affecting the system to an unacceptable extent?

In the last few decades a large number of publications have appeared on tidal asymmetry and its effects on the sediment transport and morphological development in estuaries. However, these publications are distributed over different sources and the reported studies are related to estuaries all over the world. In order to take maximum advantage of the existing

knowledge in studying the tidal waters in the Netherlands, in particular the Western Scheldt, Rijkswaterstaat commissioned WL|Delft Hydraulics to carry out the present study.

1.2 Objective of the study

The objective of the present study is

- to summarise the knowledge related to tidal asymmetry, sediment transport and morphological development in estuaries, as published in the last several decades, so as to become better accessible for studies on the Western Scheldt and other tidal water systems in the Netherlands;
- to investigate if and how the existing knowledge can be applied to the Western Scheldt estuary;
- to evaluate the significance of the tidal asymmetry to the morphological system of the Western Scheldt estuary;
- to make recommendations for further studies which will lead to a better understanding of the tidal motion and the morphological development in the Western Scheldt estuary.

1.3 Set up of the study

The study has been carried out in three steps. First a general literature survey on tidal asymmetry is carried out. The relevant and representative scientific publications on the subject have been collected and studied. Based on the literature survey the following general concepts and / or aspects are analysed and described in Chapter 2:

- the mechanisms determining the asymmetry of the horizontal tide,
- the relations between the constituents of the horizontal tides and those of the vertical tides;
- the relations between the geometry (morphology) of the estuary, or parts of it, and the asymmetry of the horizontal tide;
- the effect of the asymmetry of the horizontal tide on the bed-load and suspended load sand transport;
- the effect of the sea level rise and the 18.6-year tidal cycle on the asymmetry of the horizontal tide.

In the second step, these general concepts / aspects are investigated for the particular situation of the Western Scheldt. In other words: the knowledge (concepts, theories, etc.) are checked against the characteristics of the Western Scheldt, in order to assess their applicability to this estuary. If the answer is positive, recommendations will be made on how they can be applied; if the answer is negative recommendations will be made on how to adjust the theory, or to develop new theories.

1.4 Acknowledgement

The present study is carried out by Mrs. C. Jeuken, Prof.dr. H.J. De Vriend and Dr. Z.B. Wang from Delft Hydraulics in close co-operation with Mr. B.A. Kornman from RIKZ-RWS. The contributions of Dr.H. Gerritsen and Prof.dr.M.J.F. Stive are gratefully acknowledged.

2 General Theory

2.1 General

In this chapter the literature study concerning the general theory of tidal asymmetry and residual sediment transport is reported. In Section 2.2 the basic theory concerning tidal asymmetry and residual sediment transport is summarised. Then an analysis of the relevant concepts /aspects as mentioned in Section 1.3 is given in Section 2.3. Per concept/aspect the knowledge reported in the relevant literature is summarised and combined with some further analysis.

The term *tidal asymmetry* usually refers to the distortion of the tidal wave that makes the flood period unequal to the ebb period. If the period of water level rise is shorter then the period of water level fall, the tide is called *flood-dominant* and in the opposite case it is called *ebb-dominant*. However, in the present study tidal asymmetry is considered in relation to the morphological development via the *residual sediment transport.* Therefore the concept tidal asymmetry will be considered in a wider sense and a distinction will be made between the asymmetry of the *horizontal tide* and that of the *vertical tide*. For the vertical tide, i.e. the water level variation, the above definition of asymmetry, flood- and ebb-dominance will be adopted. The horizontal tide, by which the flow velocity (not the discharge) is meant here, will be called asymmetric if it generates a residual sediment transport. The asymmetry may be associated with a difference in the magnitude between maximum ebb and flood velocities. This type of asymmetry tends to induce a residual bed - load and suspended load transport of coarse sediment. For instance, if the maximum flood velocity exceeds the ebb velocity, a residual sediment transport in flood direction is likely to occur as the sediment transport non-linearly responds to the velocity. A second type of asymmetry that essentially affects the residual transport of fine suspended sediment is associated with a difference in the duration of slack water: a situation in which the duration of slack water before ebb exceeds the duration of slack water before flood favours a residual sediment transport in flood direction. If the residual sediment transport is in the flood-direction it will be called flood-dominant and vice versa. The residual sediment transport is the local (Eulerian) averaged sediment transport within a *tidal period*. Note that the term tidal period is often not strictly defined as the tide in reality is not periodic in the strict mathematical sense (see Appendix A). A strict definition for the period of the *vertical tide* can be the time-interval between two adjacent high waters and the period of the *horizontal tide* can be defined as the time-interval between two adjacent flood- or ebb-*slack waters*. According to these strict definitions the tidal period is variable from one tide to another. In the literature the period of the M_2 tidal constituent is often used as “the” tidal period. This latter definition is adopted in the present study as well.

The present study will focus on 1D and 2DH analyses. Three-dimensional (3D) flow structures will not be considered in detail. The study will focus on well-mixed estuaries in which the tidal motion is the major hydrodynamic driving force for the morphological

development. Thus, the river outflow is considered negligible small (like in the Western Scheldt).

2.2 Basic theory

2.2.1 Introduction

Sediment transport in estuaries is mainly caused by the water motion, which, from a large-scale point of view, is hardly affected by the sediment load. Therefore, it makes sense to analyse the water motion first, and subsequently the mechanisms which lead to the residual sediment transport.

Clearly, there can be other transport mechanisms at work in estuaries, such a the downhill gravitational transport of sand on steep slopes, or of fluid mud on much milder slopes, or man-induced transport via dredging and dumping programmes in these intensively used systems. Although these transport mechanisms may well have a significant morphological impact (cf. the morphological response of the Western Scheldt to the deepening and the maintenance of the navigation channel to Antwerp; e.g. Vroon et al., 1997), they will not be considered in this survey.

The principal forcing factors of the water motion in well-mixed estuaries like the Western Scheldt are the astronomical tide, meteorological effects and river flow. In the case of less well-mixed estuaries, the density-driven estuarine circulation should be added. The astronomical tide is usually described in terms of a number of harmonic components, of which the frequency is astronomically determined (from the motion of celestial bodies). The amplitude and phase of each component vary from place to place. The combination of these astronomical components allows us to describe a wide variety of tidal curves.

Most of the astronomical frequencies are grouped around integer numbers per lunar or solar day, but there are also low-frequency oscillations and net residual currents. In the Southern Bight of the North Sea, the strongest tidal component is the semi-diurnal lunar tide, indicated by M_2 (Moon, 2 times per lunar day). Another important semi-diurnal component is the solar tide, S_2 (Sun, 2 times per solar day). In addition, there are diurnal components, such as K_1 and O_1, which refer to the daily inequality due to the declinations of the moon and the sun.

The linear combination of two tidal components, say with frequencies ω_1 and ω_2 ($\omega_2 > \omega_1$), can easily be shown to yield an amplitude modulation of frequency $\omega_2 - \omega_1$. In terms of harmonic components, this mechanism leads to subharmonic tides (spring-neap cycle, etc.). Non-linear interactions of tidal components lead to subharmonic, as well as superharmonic tides (so-called overtides, e.g. M_4, M_6, M_8, etc., due to the interaction of M_2 with itself, but also many combined overtides, due to interactions of different components).

Non-linear interactions between tidal components are of paramount importance to the sediment transport, since they can give rise to asymmetries in the tidal velocity, which can give rise to a net (i.e. tidally averaged) sediment flux, or to a net deposition or erosion of

sediment. Therefore, part of this literature survey will be devoted to these non-linear interactions and their effects on the tidal velocity.

Another form of non-linear interaction, much underexposed in the context of sediment transport so far, is the interaction between the tide and extreme currents, e.g. due to a river flood or a storm surge. This aspect will not be considered , as the river discharge in the Western Scheldt is of minor importance.

Apart from these non-linear interactions, which can be considered as "local", as they can be explained directly from isolated terms in the mass and momentum balance equations for the flow, there are also global mechanisms that give rise to asymmetries, residual currents and or residual sediment fluxes. Some of these are associated with the propagation of tidal components in the estuary, some are topography-induced (e.g. the hypsometry effect of large intertidal shoals), others are associated with the shape of the lateral flow boundaries (e.g. the net circulation near a promontory or in the vicinity of a bend). These mechanisms will also be given due attention.

Tidal asymmetry and rectification does not only concern the velocity component in the direction of the channel axis or the mean flow. In 3-D situations, there are potentially important secondary flows that can have relatively large tidal residuals. The curvature-induced secondary flow, for instance, does not change sign between ebb and flood, so its net effect is much more important than one would guess on the basis of a comparison with the tidal main velocity amplitude.

2.2.2 Tidal asymmetry

Locally generated overtides (1-D)

The 1-D tidal motion in a prismatic straight channel of constant width is described by the following equations (see appendix B for an alternative formulation of the 1D equations):

$$\underset{(A)}{\frac{\partial u}{\partial t}}+\underset{(B)}{u\frac{\partial u}{\partial x}}=\underset{(C)}{-g\frac{\partial \zeta}{\partial x}}\underset{(D)}{-c_f\frac{u|u|}{h_0+\zeta}}+\underset{(E)}{\frac{\partial}{\partial x}\left(\nu_t\frac{\partial u}{\partial x}\right)} \tag{2.1}$$

$$\underset{(F)}{\frac{\partial \zeta}{\partial t}}+\underset{(G)}{\frac{\partial}{\partial x}\{u(h_0+\zeta)\}}=0 \tag{2.2}$$

in which:

t	=	time,
x	=	distance to channel entrance,
$u(x,t)$	=	cross-sectionally averaged flow velocity,
$\zeta(x,t)$	=	water surface elevation w.r.t. mean sea level,

h_0 = water depth below mean sea level,
ν_t = eddy viscosity,
g = acceleration due to gravity, and
c_f = bed friction factor.

The terms in the Eq. (2.1), the momentum equation, are:

(A) the local inertia term,
(B) the advective inertia term,
(C) the slope term,
(D) the bottom friction term, and
(E) the horizontal diffusion term.

The terms in Eq. (2.2), the equation of continuity, are:

(F) the storage term, and
(G) the discharge gradient term.

The local inertia term (A), the slope term () and the storage term (F) are essentially linear. In turbulent flow, the eddy viscosity in the horizontal diffusion term (E) is generally a function of the flow velocity. Hence the term term is a non-linear term. For the time being, the longitudinal velocity gradients are assumed to be so small, that the horizontal diffusion term (E) can be ignored.

Strictly speaking, the discharge gradient term, G, consist of a linear and a non-linear part:

$$\frac{\partial}{\partial x}\{u(h_0+\zeta)\}=\frac{\partial}{\partial x}\{u\,h_0\}+\frac{\partial}{\partial x}\{u\zeta\} \tag{2.3}$$

These two terms will be indicated as G1 and G2, respectively.

This leaves the advective inertia term (B), de friction term (D) and the discharge gradient term G2 as the principal sources of non-linear interaction. For clarity, some authors (e.g. Parker, 1991) split the friction term D into two parts, in order to separate the effects of the non-linear bottom friction and that of the depth variation. For small elevations as compared to the mean water depth, the following approximation can be made:

$$\frac{u|u|}{h_0+\zeta}\approx\frac{u|u|}{h_0}-\frac{\zeta\,u|u|}{h_0^2} \qquad for \qquad \frac{\|\zeta\|}{h_0}<<1 \tag{2.4}$$

The two terms in this approximation will be named D1 and D2, respectively.

Clearly, the above approximation does not hold good in every part of the Western Scheldt. It does give some insight, however, in what happens in the deeper channels.

Now let us consider a progressive tidal wave component with

$$u(x,t)=U(x)\cos(\omega t-kx) \tag{2.5}$$

in which

U = velocity amplitude,
ω = tidal frequency, and
k = tidal wave number = $2\pi/\lambda$, where
λ = tidal wave length.

Substitution into the the advective inertia term (B) yields

$$\begin{aligned} u\frac{\partial u}{\partial x} &= U\frac{\partial U}{\partial x}\cos^2(\omega t-kx)+kU^2\sin(\omega t-kx)\cos(\omega t-kx) \\ &= \underbrace{\frac{1}{2}U\frac{\partial U}{\partial x}}_{\text{rectification}} + \underbrace{\frac{1}{2}U\frac{\partial U}{\partial x}\cos 2(\omega t-kx)+\frac{1}{2}kU^2\sin 2(\omega t-kx)}_{\text{overtide}} \end{aligned} \tag{2.6}$$

Apparently, the interaction of this component with itself via the advective acceleration term induces a time-invariant effect (rectification, residual) and a superharmonic effect (overtide) of twice the basic frequency. Note that the propagation speed of this overtide is the same as that of the basic mode, viz. ω/k.

The interaction via the advective inertia term (B) of two different modes,

$$u=U\cos(\omega_1 t-k_1 x-\varphi_1)+V\cos(\omega_2 t-k_2 x-\varphi_2) \tag{2.7}$$

yields, apart from the interaction terms of each mode with itself,

$$\begin{aligned} u\frac{\partial u}{\partial x} = &\left(U\frac{\partial V}{\partial x}+V\frac{\partial U}{\partial x}\right)\cos(\omega_1 t-k_1 x-\varphi_1)\cos(\omega_2 t-k_2 x-\varphi_2)+ \\ &UV\left[k_2\cos(\omega_1 t-k_1 x-\varphi_1)\sin(\omega_2 t-k_2 x-\varphi_2)+\right. \\ &\left.k_1\sin(\omega_1 t-k_1 x-\varphi_1)\cos(\omega_2 t-k_2 x-\varphi_2)\right] \end{aligned} \tag{2.8}$$

or, after some elaboration,

$$\begin{aligned} u\frac{\partial u}{\partial x} = &\frac{1}{2}\left(U\frac{\partial V}{\partial x}+V\frac{\partial U}{\partial x}\right)\left[\cos\{(\omega_1+\omega_2)t-(k_1+k_2)x-(\varphi_1+\varphi_2)\}+\right. \\ &\left.\cos\{(\omega_1-\omega_2)t-(k_1-k_2)x-(\varphi_1-\varphi_2)\}\right]+ \\ &UV\left[\frac{k_1+k_2}{2}\sin\{(\omega_1+\omega_2)t-(k_1+k_2)x-(\varphi_1+\varphi_2)\}+\right. \\ &\left.\frac{k_1-k_2}{2}\sin\{(\omega_1-\omega_2)t-(k_1-k_2)x-(\varphi_1-\varphi_2)\}\right] \end{aligned} \tag{2.9}$$

So, in general, the interaction of two modes via the advective acceleration term yields two types of additional components, one with a frequency equal to the sum of the frequencies of the basic modes and one with a frequency equal to the difference of those frequencies. The propagation speeds of these non-linearly generated modes generally differ from those of the basic modes:

$$\frac{\omega_1-\omega_2}{k_1-k_2} \quad and \quad \frac{\omega_1+\omega_2}{k_1+k_2} \quad instead\ of \quad \frac{\omega_1}{k_1}=\frac{\omega_2}{k_2}$$

The non-linear interaction via the discharge gradient term, G2, concerns combinations of velocity and the water surface elevation. Since the frequencies and the wave numbers of the two are coupled, this interaction has the same type of effects as the one via the B-term, viz. the generation of modes with frequencies equal to the sum and the difference of the basic frequencies. Self-interaction of modes therefore yields a mean flow (zero frequency) and a mode with twice the basic frequency.

The Fourier decomposition of the friction terms D1 and D2 is not quite straightforward, because they include the velocity modulus. Le Provost (1991) gives an overview of recent literature on this subject. For a single component, $u|u|$ can be decomposed as follows:

$$u|u|=U^2\sum_{n=0,1,2,\ldots}(-1)^{n+1}\frac{8}{(2n-1)(2n+1)(2n+3)\pi}\cos(2n+1)\omega t \qquad (2.10)$$

This means that self-interaction via the D1-term generates odd superharmonics (3, 5, ... times the basic frequency), such as M_6. Moreover, *n=0* in the above expression yields a contribution at the basic frequency, which corresponds with the energy dissipation from the basic mode by bottom friction.

The non-linear interaction via the D2-term is due to the triple product $\zeta u|u|$. This induces mean-flow contributions and even superharmonics, such as M_4, as can be seen by multiplying the series equation (2.10) with *cosωt*:

$$\begin{aligned}
n=0 \ \Rightarrow \quad & \cos\omega t\cos\omega t=\frac{1}{2}+\frac{1}{2}\cos 2\omega t\\
n=1 \ \Rightarrow \quad & \cos\omega t\cos 3\omega t=\cos\omega t\left(4\cos^3\omega t-3\cos\omega t\right)\\
& =4\cos^4\omega t-3\cos^2\omega t\\
& =\frac{4}{4}\left(1+2\cos 2\omega t+\cos^2 2\omega t\right)-\frac{3}{2}\left(1+\cos 2\omega t\right)\\
& =\frac{1}{2}\cos 2\omega t+\frac{1}{2}\cos 4\omega t
\end{aligned}$$

Table 2.1, after Parker (1991), gives an overview of the tidal constituents that are generated by the non-linear interaction of M_2 with itself and a number of other astronomical constituents.

Clearly, the interaction of M2 with other components via the $u|u|$-term (D1) generates a set of compound constituents which differs from the ones generated by the other non-linear terms. Proudman (1923, 1955) has already pointed out that the quadratic friction term is able to generate compound tides with a frequency $2\omega_{M2} - \omega_C$, as shown in Table 2.1.

Table 2.1: Compound tide and overtide constituents generated by interaction with M_2 via the various non-linear (NL) terms.

M_2 interacting with (C) ⇓	generates tidal constituents with frequency				
	$\lvert\omega_{M2} - \omega_C\rvert$	$(2\omega_{M2} - \omega_C)$	$(\omega_{M2} + \omega_C)$	$(2\omega_{M2} + \omega_C)$	$(4\omega_{M2} - \omega_C)$
itself	mean	M_2	M_4	M_6	M_6
N_2	MN (Mm)	$2MN_2$ (L_2)	MN_4	$2MN_6$	$4MN_6$
S_2	MS (MSf)	$2MS_2$ (μ_2)	MS_4	$2MS_6$	$4MS_6$
K_1	MK_1 (O_1)	$2MK_3$ $2MO_3$	MK_3	$2MK_5$	$4MK_7$
O_1	MO_1 (K_1)		MO_3	$2MO_5$	$4MO_7$
NL-terms responsible	B D2 G2 D1[1]	D1	B D2 G2 D1[1]	D1	D1

Moreover, the Fourier decomposition of the D1-term also reveals that the co-existence of various constituents leads to an additional loss of energy from each constituent. From the point of view of M_2, this works either way: M_2 draws a substantial amount energy from the other constituents, but the others also draw a non-negligible amount of energy from M_2 (cf. Le Provost and Fornerino, 1985). This is a point to be taken into account when calibrating a tidal model which describes only M_2 against data from a composite tide: one is tempted to take the friction coefficient larger than it should be. This also applies to the interactions of the tide with a steady current or a low-frequency storm surge. The presence of a strong river flow, for instance, is known to reduce the amplitude of the tide as it propagates up the estuary (cf. Parker, 1991).

A comprehensive literature survey on local non-linear tidal interaction mechanisms is given in chapter 3 of the book “Tidal Hydrodynamics”, edited by B.B. Parker (1991). Apart from several review articles, it contains a number papers focusing especially on the role of the friction term.

So far, we have only considered purely progressive tidal waves. In reality, the tidal motion at a given frequency usually consists of two waves propagating in opposite directions. This can be generalised to

[1] *via interaction with the mean flow*

$$\begin{aligned}\zeta_n(x,t) &= \hat{\zeta}_n^+(x)\cos(\omega_n t - k_n x - \varphi_n^+) + \hat{\zeta}_n^-(x)\cos(\omega_n t + k_n x - \varphi_n^-) \\ &= \mathrm{Re}\left\{H_n(x)e^{i\omega_n t} + H_{-n}(x)e^{-i\omega_n t}\right\} \quad for \quad n = 1,2,3,.....\end{aligned} \tag{2.11}$$

and

$$\begin{aligned}q_n(x,t) &= q_n^+(x)\cos(\omega_n t - k_n x - \psi_n^+) + q_n^-(x)\cos(\omega_n t + k_n x - \psi_n^-) \\ &= \mathrm{Re}\left\{Q_n(x)e^{i\omega_n t} + Q_{-n}(x)e^{-i\omega_n t}\right\} \quad for \quad n = 1,2,3,....\end{aligned} \tag{2.12}$$

In the case of a purely progressive wave, $H_n = H_{-n}$; in the case of two combined waves propagating in opposite directions, $H_n \neq H_{-n}$.

Using the above generalisation, Dronkers (1964) formulates mass and momentum equations per constituent. This leads to a set of ordinary differential equations in *x*, with the amplitude functions in the above expressions as dependent variables. Due to the non-linearities in the model (Dronkers also includes a depth-dependent channel width), these equations are coupled. This shows the impossibility to single out a model of one tidal component, at least in the case of a non-linear tide.

2.3 Analysis of relevant aspects

2.3.1 Mechanisms determining asymmetry of horizontal tide

The term horizontal tide refers to the flow velocity here, since the sediment transport is related to the flow velocity, rather than the discharge. The horizontal tide will be considered as asymmetric if it induces a residual sediment transport within a tidal period. The relation between the residual sediment transport and the horizontal tide is discussed in Section 2.3.4. The works of Van de Kreeke & Robaczewska (1993) and Groen (1967) show that the residual flow velocity, as well as the high-frequency harmonics (quarter-diurnal, sixth-diurnal, … overtides) of the flow velocity can contribute to residual sediment transport. Therefore both aspects will be considered here.

Residual flow

Processes and mechanisms influencing the residual flow velocity in a well-mixed estuary are the upstream river discharge, wind and the tidally induced horizontal circulation. The residual flow velocity due to the upstream river discharge will not be considered in the present study, since it is of minor importance in the Western Scheldt. In estuaries where the upstream river discharge plays a significant role, it can easily become the dominating factor determining the residual sediment transport, thus reducing the *tidal* asymmetry to a factor of secondary importance. Wind induced circulation will only be considered only briefly.

Tidally induced residual flow is a difficult subject to be studied. It is very sensitive to geometry and bathymetry (Zimmerman, 1978, 1980, 1981, Ridderinkhof, 1988a, 1988b, 1989). This makes the result from a study for a particular case difficult to be applied to other cases. However, there are still general principles on the qualitative features of the tidally

induced circulation which seem to be universally applicable. Two types of circulation may be distinguished: the (horizontal) geometry-induced circulation (e.g. by an irregular shoreline) and the bathymetry induced circulation (Fig.2.1). A typical example of the first type is the circulation induced by headland. A general principle for the bathymetry-induced circulation is that in the relatively deep parts the residual flow tends to be in the ebb-direction and in relative shallower parts it tends to be in the flood -direction. If a cross-section of an estuary is bimodal, i.e. with two channels, the residual flow in the deeper channel is usually in the ebb-direction, whereas in the shallower part it is in the flood-direction (Van Veen, 1950, Kjerfve, 1978).

Fig2.1 Geometry induced (left) and bathymetry induced (right) circulation. In both cases the estuary/embayment has a finite length.

The non-linear advection term representing the inertia in the momentum equation appears to be more important for the residual flow than one might expect on the basis of the (relative) order of magnitude of this term. This has been shown by Zimmerman (1978, 1980, 1981, see also Ridderinkhof, 1989) using the (tidally averaged) vorticity-equation.

According to Tee (1976) tides may generate residual currents through:

- nonlinear bottom friction,
- the non-linear terms in the continuity equation, and
- the nonlinear advective terms in the momentum equation.

The last one is found to be the most important one in his case (Bay of Funday, USA), even though it has only a minor influence on the vertical tide. In the Bay of Fundy the geometry-induced circulation is the most important.

Li and O'Donnell (1998) give an explanation of the flood-dominance in relatively shallower parts and the ebb-dominance in relatively deeper parts of the cross-section. They use an analytical solution of the residual current for a prismatic shallow estuary with a cross-section as shown in Fig.2.2. They show that the residual circulation, with flood-directed flow on the two shallow banks and ebb-directed flow in the deeper central part, is the result of a competition among several processes. An inward (flood) flux is caused by local non-linearity, both in the bottom friction and in the propagation (advective term) of the finite-amplitude tidal wave. This inward flux is larger on the shoals and smaller in the channel due to the stronger non-linearity in the shallower water. The residual inward flow creates a set-up (residual surface elevation) of water at the head of the estuary that produces a pressure gradient. This pressure gradient is approximately uniform across the estuary and drives an outward flow that is larger in the channel centre than on the shoals. In this particular case, the non-linear bottom friction appears to be much more important than the advective term.

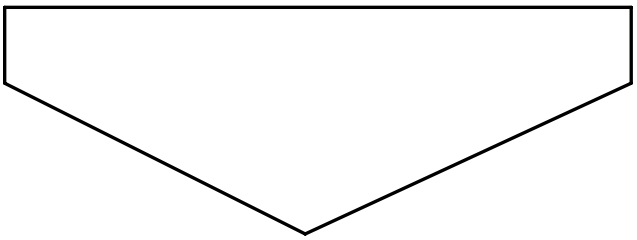

Fig.2.2 Schematic cross-section used by Boon (1988)

Apparently, the inertia effect (non-linear advective term) is the major source of the (horizontal) geometry-induced residual circulation, whereas for the bathymetry-induced circulation the non-linear friction is the major source. Residual circulation in estuaries is usually a combination of the two types.

By averaging the numerically calculated water levels and current velocities in the Western Wadden Sea, Ridderinkhof (1988a) shows that the tidally driven residual current velocity field is composed of isolated residual eddies and a through-flow between the different basins. The residual velocities associated with the eddies are one order of magnitude larger than the residual velocities associated with the through-flow. The residual flow field calculated with the DETWES model for the Western Scheldt (Van der Male, 1993, see also Vroon et al, 1997) shows the same features: eddies at the scale of the flood- and ebb-channel systems and within wide channels dominate the pattern of the residual flow field. Van der Kerckhoven (1995) shows that the schematisation of the width variation of the branches in a 1D network model is important for reproducing the correct circulation in a flood- and ebb-channel system. A correct reproduction of the residual flow with the existing 1D-network schematisation appears only possible if the roughness coefficient is made dependent on the flow-direction and variable from channel to channel (especially the difference in value between flood-channels and ebb-channels is important; see Fokkink, 1998).

2.3.2 Asymmetry of horizontal tide and vertical tidal constituents

The relation between the asymmetry of the horizontal tide and the vertical tidal constituents can be analysed in two steps. First the relation between the asymmetry of the vertical tide and the tidal constituents is analysed. Then the relation between the asymmetry of the horizontal tide and that of the vertical tide is discussed.

Tidal asymmetry and tidal constituents of the vertical tide

The asymmetry of the vertical tide usually refers to the distortion of the (predominant) semi-diurnal tide due to the (quarter-diurnal, sixth-diurnal, …) overtides. The strength of the asymmetry depends on the ratio between the amplitude of the overtide and that of the semi-diurnal tide, and the nature of the asymmetry (ebb or flood dominance) is determined by the phase difference between the overtide and the semi-diurnal tide. Take for example the asymmetry caused by the quarter-diurnal tide. Flood-dominance (water level rises faster than it falls) occurs if the phase difference is between 0^o and 180^o, otherwise ebb-dominance occurs. Here it is assumed, however, that the semi-diurnal tide is described by a single harmonic function, and that the same goes for the quarter-diurnal tides, etc. This is not the case in reality. In other words, this reasoning only applies if the tide is described by a Fourier

series with a semi-diurnal base-period. However, such a Fourier series is in fact modulated in time, due to e.g. the spring-neap variation. This raises the question whether the tidal asymmetry is also time-varying.

The water elevation at a certain location can be written as:

$$\zeta(t) = \sum_i f_i a_i \cos\left(\omega_i t - \varphi_i - \vartheta_i\right) \tag{2.13}$$

with

f	=	astronomical constant,
a	=	amplitude,
ω	=	frequency,
φ	=	phase,
ϑ	=	astronomical phase.

As an example the most important semi-, quarter- and sixth-diurnal constituents at the Vlissingen station derived from the data of 1997 are depicted in Fig.2.3. There is more than one semi-diurnal constituent and the same goes for the quarter-diurnal constituents, etc.

Speer et al (1991) observes that the relative phase-difference between the quarter-diurnal constituents and their semi-diurnal parent constituents is about the same for all constituents at the same station, thus

$$2\varphi_{M2} - \varphi_{M4} \approx \varphi_{M2} + \varphi_{N2} - \varphi_{MN4} \approx \varphi_{M2} + \varphi_{S2} - \varphi_{MS4} \tag{2.14}$$

Based on this observation they argue that the nature of the tidal asymmetry can be represented by the phase difference between the M_4 and the M_2 constituents.

The temporal variation of tidal asymmetry has been studied by Boon (1988) using the complex demodulation method. This actually implies that the Fourier series with a semi-diurnal base-period is analysed with a moving time interval, in order to find the temporal variation of a_4/a_2 and $2\varphi_2-\varphi_4$. He applied the analysis to a predicted time series of the tidal level and to the observed time series (see Fig.2.4). The results show that

- both parameters indicating the tidal asymmetry are time-varying, although the predicted and observed tides do not give exactly the same results;
- the mean values of the two parameters are indeed about the same as when computed for the M_2 and M_4 tides only. This supports the arguments of Speer et al (1991);

Fig.2.3 Tidal constituents at Vlissingen (1997)

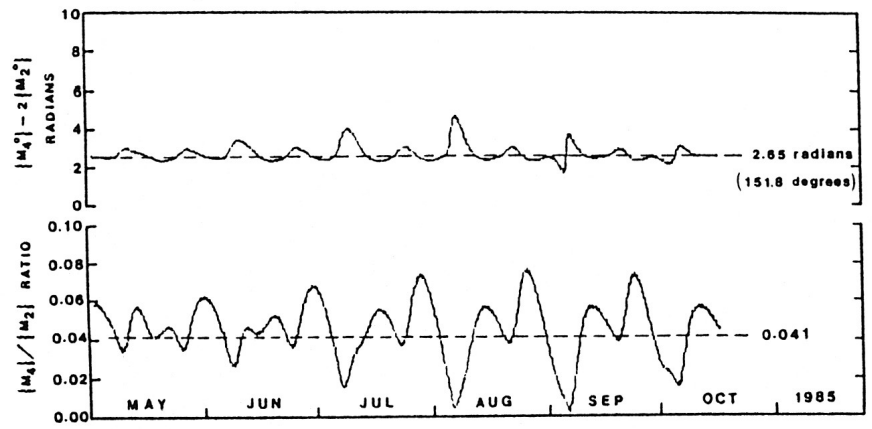

Amplitude ratios $\{M_4\}/\{M_2\}$ and phase differences $\{M_4^*\}-2\{M_2^*\}$ computed using complex demodulation of predicted tides, Wachapreague, Virginia.

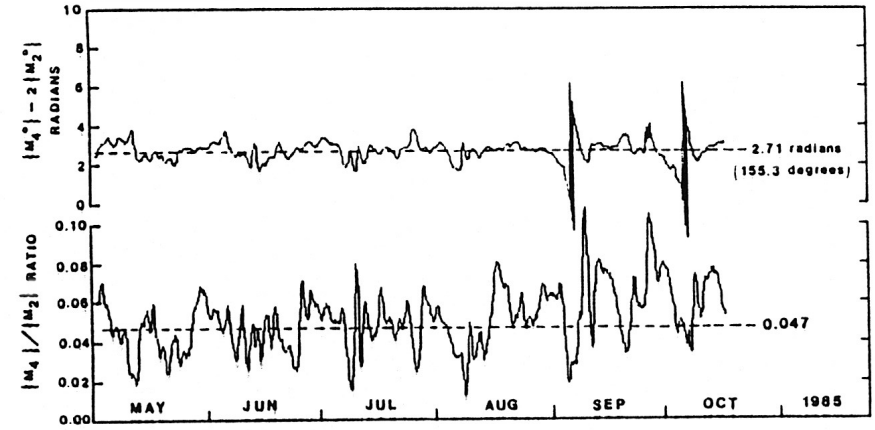

Amplitude ratios $\{M_4\}/\{M_2\}$ and phase differences $\{M_4^*\}-2\{M_2^*\}$ computed using complex demodulation of observed tides, Wachapreague, Virginia.

Fig.2.4 temporal variation of the distortion parameters (after Boon, 1988)

For known tidal constituents, the analysis of the temporal variation of the tidal asymmetry can actually be carried out in a much simpler way. Within a tidal period, which is relatively small at the time scale of the spring-neap variation, all semi-diurnal constituents can be approximated as having the same frequency. Each constituent can then be represented by a complex number with the amplitude as a modulus and the phase at that moment as a phase angle. The combined semi-diurnal tide is then simply obtained by summing up all the constituents:

$$a_2 \exp(i\varphi_2) = f_{M2} a_{M2} \exp(i\varphi_{M2} + i\vartheta_{M2}) + f_{N2} a_{N2} \exp(i\varphi_{N2} + i\vartheta_{N2}) + f_{S2} a_{S2} \exp(i\varphi_{S2} + i\vartheta_{S2}) + \cdots \quad (2.15)$$

The same can be done for the quarter-diurnal tide, etc. In this way the parameters determining the tidal asymmetry can be obtained without going through the production of a time series. The results of this analysis using the tidal constituents of Vlissingen are shown

in Fig.2.5 for the quarter-diurnal tide and Fig.2.6 for the sixth-diurnal tides. In these figures the two parameters determining the tidal asymmetry are depicted as functions of the amplitude of the combined semi-diurnal tide, so the spring-neap variation can clearly be observed. Each dot in the figures represents the beginning of one day (00:00:00) in the year 1999. The following observations are made:

- The amplitude ratio of the tidal asymmetry increases with the amplitude of the tide. Thus at spring tide the asymmetry is much stronger than at neap tide.
- The averaged phase difference agrees with that between the M_2 tide and its over tides (M_4 and M_6).
- Between the averaged tide to the spring tide the scatter of the phase difference is relatively small but near neap tide the scatter is much larger.

A closer observation learns that

- The phase difference is larger in the period from spring to neap than in the period from neap to spring. In other words, in the cycle spring-neap-spring the path followed by the phase difference first follows the upper edge of the envelope of scatter, then undergoes a sharp drop at neap tide and finally follows the lower edge.
- The amplitude ratio is larger in the period from spring to neap than in that from neap to spring.

The sharp variation of the phase difference at neap tide, which has also been observed by Boon (1988), seems strange but can be explained by considering the combination of M_4 and MS_4. As demonstrated in Fig.2.7 the difference between this combined tide and the M_4 tide over a complete spring-neap cycle can be represented as a point describing a circle in the complex plane. The centre of the circle represents the M_4-tide and the radius the amplitude of the MS_4-tide. The angle of the vector from the centre point at the circle is the phase difference between M_4 and MS_4. This angle increases linearly with time. The angle between the horizontal axis and the line connecting the origin at and the point at the circle is the phase difference between the combined tide and M_4. If the amplitude of M_4 and MS_4 are about the same, as in the case of the Vlissingen station, this angle varies sharply at neap tide, as is demonstrated by the figure.

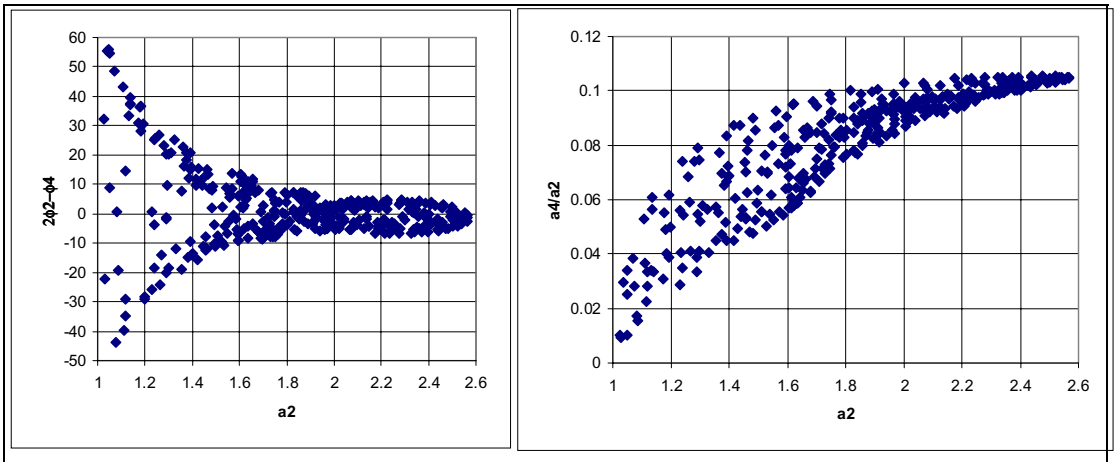

Fig2.5 Predicted amplitude ratio and phase difference between semi- and quarter-diurnal tides at Vlissingen

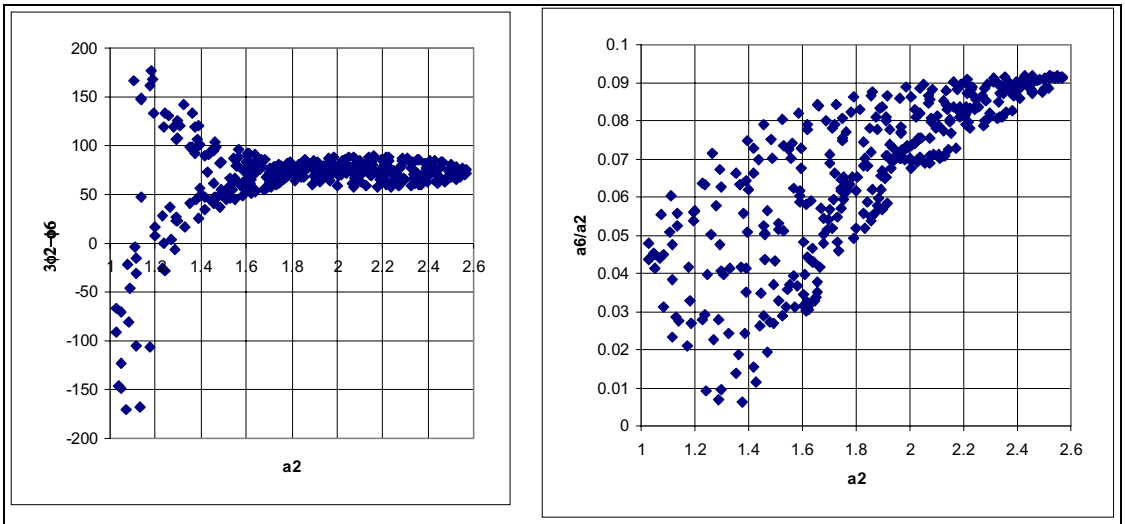

Fig2.6 Predicted amplitude ratio and phase difference between semi- and sixth-diurnal tides at Vlissingen

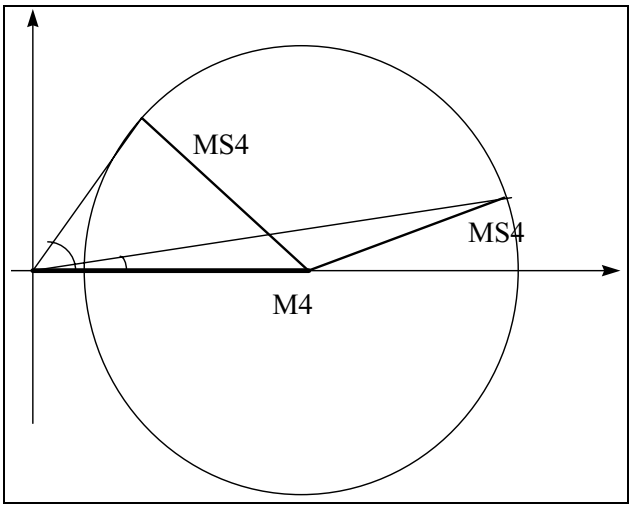

Fig.2.7 Representation of the difference between the combined tide MS_4 and the M_4 tide over a complete spring-neap cycle (for explanation see text).

Asymmetry of horizontal tide

The horizontal tide is closely related to the vertical tide as can be demonstrated by applying the continuity equation. For an arbitrary section of the estuary, the following relation between the water elevation and the discharge applies:

$$Q_1 - Q_2 = \int_{x_1}^{x_2} b(x,\zeta)\frac{\partial \zeta}{\partial t}\,dx \qquad (2.16)$$

Herein

Q_1 = discharge at x_1
Q_2 = discharge at x_2
b = storage width

It is clear that asymmetry in the vertical tide will directly cause asymmetry in the horizontal tide. However, the relation between the horizontal tide and the vertical tide is not a simple linear one. Equation (2.16) is non-linear because the storage width depends on the water level. Furthermore, another source of non-linearity of the flow velocity is the dependency of the cross-sectional area on the water level:

$$u(t) = \frac{Q(t)}{A(\zeta(t))} \tag{2.17}$$

Fry and Aubrey (1990) have analysed the non-linear relation between the distortion parameters (amplitude ratio and the phase difference between quarter-diurnal and semi-diurnal tides) of the flow velocity and those of the water level. They concluded that the non-linear relations are quite different from the linear ones, although in their particular case the differences in the two parameters do not cause significant differences in the resulting bed-load transport because they cancel out.

2.3.3 Relations between morphology and tidal asymmetry

Concerning the relation between the morphology in the estuary and the tidal asymmetry, two aspects need to be discussed, viz. the influence of the morphology on the tidal asymmetry and the influence of the tidal asymmetry on the morphological development.

Influence of morphology on tidal asymmetry

The influence of the morphology on the tidal asymmetry is unambiguous in the sense that, given the morphology of the estuary, the tidal motion and thus also the tidal asymmetry in the estuary is determined entirely by the external forcing (tide at the open sea). The relevant morphological parameters for the tidal motion are the width and depth as shown by the governing equations described in Section 2.2. Actually a distinction needs to be made between the stream width and the storage width. Furthermore the roughness coefficient is also influenced by the depth (the hydraulic radius) and the micro-morphology (bed-forms).

Speer and Aubrey (1985) and Friedrichs and Aubrey (1988) studied the influence of geometry and bathymetry of short, friction-dominated and well-mixed estuaries using 1D numerical models. They conclude that the parameters determining the tidal asymmetry in such an estuary are

- the ratio of the tidal amplitude and the mean water depth, a/h, and
- the ratio of the volume of water stored between low and high water in tidal flats and marshes and the volume of water contained in the channels below mean sea level V_s/V_c.

Relatively shallow estuaries tend to be flood-dominant and estuaries with relatively more intertidal flats tend to be ebb-dominant. Based on the results of Friedrichs and Aubrey (1988), Speer et al. (1991) constructed the graph in Fig. 2.9, which shows the influence of the two parameters on the tidal asymmetry of the vertical tide.

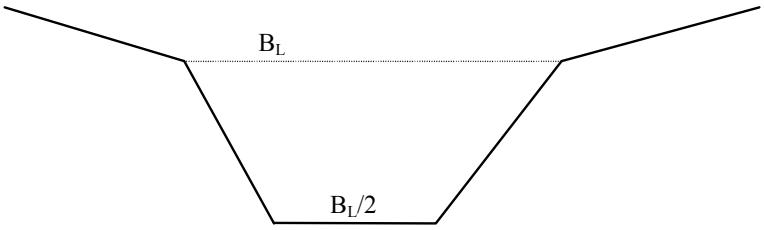

Fig2.8 cross-section used in the model of Speer and Aubrey (1985)

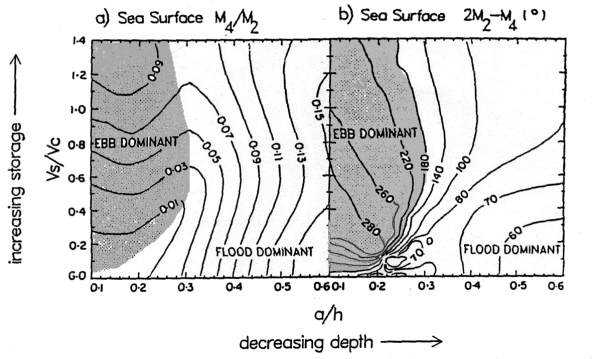

Fig.2.9 Contour plots of the parameters that determine nonlinear distortion as a function of a/h and V_s/V_c, resulting from 84 model systems. The 180° contour separates the plots into flood- and ebb-dominant regions (After Speer et al., 1990)

The graphs in Figure 2.9 show that beyond a certain value of V_s/V_c, the ebb- or flood-dominance almost exclusively depends on *a/h*. Under such circumstances an increase of the water depth h results in a shift towards ebb-dominance. When this ebb-dominance is associated with an export of sediment, a positive feedback occurs that may lead to a drowning of the system. Likely wise, the opposite situation, i.e. flood dominance and in-filling, may also occur.

Note that they used a fixed length of the estuary and all cases considered are friction-dominated. For the more general cases Li and O'Donell (1995) showed that the following additional parameters may also influence the residual flow (circulation) and hence the tidal asymmetry:

- the ratio of the length of the estuary and the tidal wave length,
- the ratio of a length-scale of the morphological variation along the estuary (e.g. the change of the width) and the tidal wave length,
- the ratio of the tidal period and the decay time scale due to friction.

Dronkers (1986, 1998) also claims that the inter-tidal area in the estuary is a very important parameter. Based on an analytical solution of the tidal propagation in semi-enclosed basins, he comes to the conclusion that

$$\Delta t_{flood} - \Delta t_{ebb} \propto H^- H_k^- - H^+ H_k^+ \tag{2.18}$$

with

Δt_{flood} = flood period at the mouth
Δt_{ebb} = ebb period at the mouth
H_k = A/b, cross-sectional area divided by storage width
H = water depth

and the superscripts + and - representing high and low water, respectively.

Tidal asymmetry is the result of the deformation of the tidal wave during propagation. In general a symmetric tide will be deformed into a flood-dominant tide if the high water propagates faster than the low water and vice versa. This simple general rule can be used to understand the relation between the morphology and the tidal asymmetry. If the effect of the roughness term is neglected the propagation speed of tidal wave is (Dronkers, 1964):

$$c = \sqrt{g\frac{A}{B}} \tag{2.19}$$

with

c = propagation speed
g = gravitational acceleration
A = cross-sectional area
B = storage width

According to this equation the propagation speed of the high water will be equal to that of the low water if

$$\frac{A_H}{A_L} = \frac{B_H}{B_L} \tag{2.20}$$

where the subscripts H and L represent the high and low water, respectively. Following the schematisation of Speer and Aubrey (1985, also see Fig. 2.8), we have

$$\frac{A_H}{A_L} = 1 + \frac{8}{3}\frac{\frac{a}{H}}{1-\frac{a}{H}} \tag{2.21}$$

$$\frac{V_s}{V_c} = \frac{(B_H - B_L)a}{\frac{3}{4}B_L H + \frac{1}{4}B_L a} \qquad \text{thus} \qquad \frac{B_H}{B_L} = \frac{V_s}{V_c}\frac{H}{a}\left(\frac{3}{4} + \frac{1}{4}\frac{a}{H}\right) + 1 \tag{2.22}$$

Equation (2.20) then becomes

$$\frac{V_s}{V_c} = \frac{2\frac{a}{H} + \frac{8}{3}\frac{\left(\frac{a}{H}\right)^2}{1-\frac{a}{H}}}{\frac{3}{4} + \frac{1}{4}\frac{a}{H}} \tag{2.23}$$

This equation is depicted in Fig.2.10. When compared with the numerical results of Speer et.al. (1990) and Speer & Aubrey (1985) (Fig.2.9), the qualitative agreement is evident : the approximate ranges of V_s/V_c and a/h for which the vertical tide is ebb or flood-dominant more or less coincide.

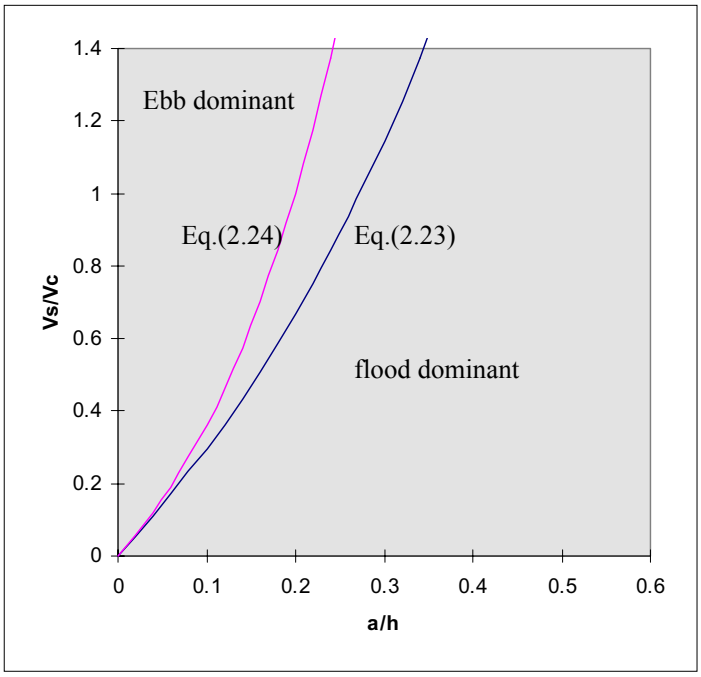

Fig2.10 Ebb-flood dominance of the vertical tide as a function V_s/V_c and a/h according to the formulation derived in equation 2.23 and that of Dronkers (1998, equation 2.24). In the derivation of the equation and the schematisation of Speer and Aubrey (1985) was applied.

It is also noted that according to the relation derived by Dronkers (1998) the flood period and ebb period will be equal in the case considered by Speer et al (1991) if

$$\frac{V_s}{V_c} = \frac{2\frac{a}{H} + \frac{8}{3}\frac{\left(\frac{a}{H}\right)^2}{1-\frac{a}{H}}}{\frac{3}{4} + \frac{1}{4}\frac{a}{H}} \frac{1+\frac{a}{H}}{1-\frac{a}{H}} \tag{2.24}$$

This relation is shown in Fig.2.10 as well. It very resembles equation 2.23 and the graphs given by Speer et.al. 1991.

Influence of tidal asymmetry on morphology

Tidal asymmetry has a strong influence on the residual sediment transport, so it must be important for the morphological development in estuaries. The nature of the tidal asymmetry can determine the direction of the sediment flux. For the Western Scheldt there seems to be a correlation between the asymmetry of the vertical tide and the sediment flux between the various parts of the estuary derived from the sand balance (Gerritsen et al, 1999). This indicates that the tidal asymmetry is an important factor influencing the mega-scale morphological development. However, it is noted that tidal asymmetry is one of the many influencing factors. This means that knowledge on the tidal asymmetry alone is not sufficient to predict morphological changes. In this sense the influence of the tidal asymmetry on the morphological development is not exclusive. Furthermore, tidal asymmetry probably plays a relatively less important role in the morphological development at smaller scales, e.g. the development of tidal flats governed by meso-scale processes like the sediment exchange between flat and channel. On the other hand, it is the tidal flat that is important to the tidal asymmetry. Predictions of future morphological developments can therefore not be based on the interaction between morphology and tidal asymmetry alone.

2.3.4 Effect of tidal asymmetry on sediment transport

Two types of sediment transport have to be distinguished for discussing the effect of tidal asymmetry on the residual sediment transport, viz. bed-load transport and suspended load transport. The bed-load transport rate is considered to be directly related to the local instantaneous flow velocity, whereas the suspended-load transport rate also depends on the flow condition upstream and in the past, because of the relaxation effect of the suspended sediment concentration.

For the bed-load transport the work of Van de Kreeke and Robaczewska (1993) gives a clear insight into the effect of the asymmetry of the horizontal tide on the residual transport. Assuming the flow velocity to be dominated by M_2 tide and the bed-load transport to be proportional to a power of the local current velocity, they show that the long-term mean bed-load transport only depends on the residual flow velocity M_0, the M_2 components and its overtides (M_4, M_6). This is demonstrated using the following expression for flow velocity:

$$u(t) = u_0 + \hat{u}\cos(\omega t) + \sum_i u_i \cos(\omega_i t - \varphi_i) \qquad (2.25)$$

in which

u	=	flow veocity
t	=	time
u_0	=	residual flow velocity
$\hat{u}$	=	amplitude of the M_2 tidal current
ω	=	angular frequency of the M_2 tide
u_i	=	amplitude of other tidal current constituents

ω_i = angular frequency of other tidal constituents
φ_i = phase of other tidal current constituents

In their analysis the K_1, S_2, N_2, M_4, M_6, and MS_4 are included as the other constituents in equation (2.25). If, for example, the following sediment transport formulae is used,

$$s = fu^3 \tag{2.26}$$

the long-term averaged transport is given by

$$\frac{\bar{s}}{f\hat{u}^3} = \frac{3}{2}\frac{u_0}{\hat{u}} + \frac{3}{4}\frac{u_{M4}}{\hat{u}}\cos\varphi_{M4} + \frac{3}{2}\frac{u_{M4}}{\hat{u}}\frac{u_{M6}}{\hat{u}}\cos\left(\varphi_{M4} - \varphi_{M6}\right) \tag{2.27}$$

Thus only the residual flow velocity and the overtides of M_2 are important for the long-term averaged bed-load transport rate, in which long-term refers to a time scale much larger than the modulation periods associated with the combinations with other constituent. The other constituents only cause fluctuations of the residual sediment transport rate at frequencies that are associated with the beat frequency of M_2 and the corresponding constituent. The S_2 tidal current, for instance, causes a spring-neap variation of the residual transport rate, and the same does the MS_4 constituent.

Van de Kreeke and Robaczewska (1993) noticed that equation (2.27) shows that the statement in the literature (e.g. Fry and Aubrey, 1990) that the tidal-current constituents M_6, M_{10} etc. do not contribute to the tidally averaged bed-load transport is not true.

Van de Kreeke and Robaczewska's (1993) conclusions so far are universally applicable. With a numerical model of the Ems Estuary they also show that, for producing the M_0, M_2, M_4 and M_6 constituents, it does not make any significant difference whether only these constituents are prescribed at the open sea boundary, or the complete set of astronomical constituents. This implies that for morphodynamic modelling a cyclic tide with M_2 tide and its overtides will be sufficient. The general applicability of the latter conclusion is not sufficiently demonstrated and therefore its validity should be considered for each particular case.

Equation (2.27) also shows that the residual bed-load transport due to the overtides depends on the phases of these overtides relative to that of M_2, which determine not only the magnitude but also the direction of the residual transport. This can simply be interpreted as that the residual bed-load transport is in the direction of the largest current-speed due to the strongly non-linear relation between bed-load transport and flow velocity. It is noted that the threshold of sediment motion tends to enhance the effect of the velocity asymmetry.

This mechanism applies also to the suspended transport. However, for the suspended transport there is also an additional mechanism which can cause residual transport in cases where the residual bed-load transport is zero. This is illustrated by Groen (1967) using the following simple model for the relaxation effect in the sediment concentration:

$$\frac{\partial c}{\partial t} = \frac{c_e - c}{T_a} \tag{2.28}$$

where

c	=	depth averaged sediment concentration
c_e	=	equilibrium value of c (depending on the instantaneous velocity
T_a	=	adaptation time

An example of the solution of this equation is shown in Fig.2.11, illustrating that a residual suspended transport will occur in a case where there is no residual bed-load transport. The residual transport is flood-directed if the high-water slack is longer than the low-water slack and vice versa.

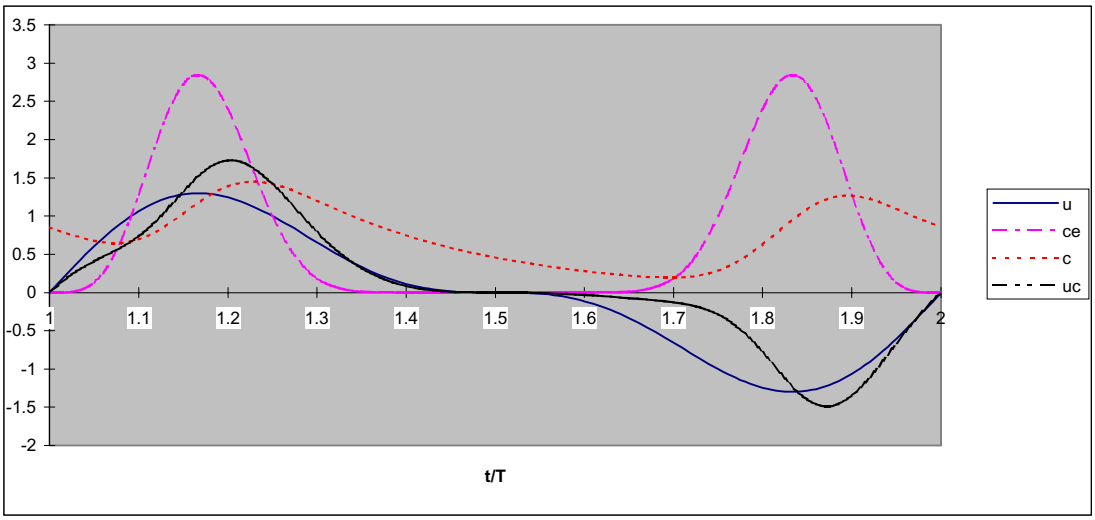

Fig.2.11 The effect of lag effects on the residual suspended sediment transport.

2.3.5 Effect of sea-level rise and 18.6 year tidal cycle on tidal asymmetry

The relation between the morphology and the tidal asymmetry, as discussed in 2.3.3, can be applied to analyse the impact of the sea-level rise and the 18.6-yearly tidal cycle on the tidal asymmetry. A changed mean sea level and/or a change in tidal amplitude cause a change of the morphological parameters influencing the tidal asymmetry, and thus a change in the tidal asymmetry. An analysis on the impact of sea-level rise has been carried out by Friedrichs et al (1990) using the theory developed by Speer and Aubrey (1985). They concluded that the reaction of an estuary to sea-level rise depends on the local estuarine geometry. Some systems will fill in faster (relatively more sediment import) as sea-level rises, whereas others will flush more efficiently (more export). This means that the response of any individual estuary requires careful assessment.

Based on the results of Friedrichs et al (1990), Louters (1998) made an analysis for the Western Scheldt case and concluded that under influence of accelerated sea-level rise the tide in the Western Scheldt will tend to become more ebb-dominant. The following remarks are made on this conclusion:

- The analysis of Friedrichs et al (1990) and that of Speer and Aubrey (1985) concern relatively small estuaries, much smaller than the Western Scheldt. It is not known if their conclusions can directly be applied to the Western Scheldt. Gerritsen et al (1999) shows that the results of Speer and Aubrey (1985, see also Speer et al, 1991) cannot be applied to the Western Scheldt in a quantitative sense, but that they can be applied qualitatively to explain the tendency of the developments. In Chapter 3 the applicability of these theories to the Western Scheldt will be discussed in further depth.
- The time scale of sea-level rise is in the order of centuries and that of the 18.6-yearly cycle is obviously decades. At such time scales the morphological development of the estuary under consideration cannot be ignored. This means that a complete analysis of the impacts of these variations should include the interaction with the morphological development. This will make the analysis very complicated, which probably explains why the studies reported in the literature insufficiently include this aspect.

3 Tidal asymmetry in the Western Scheldt

3.1 Introduction

This chapter aims to evaluate the previously discussed theoretical concepts and aspects of tidal asymmetry for the Western Scheldt estuary (Fig.3.1). For this purpose the available results of morphologic and hydrodynamic observations (and numerical modelling) are used to investigate and elaborate on:

- The mechanisms that generate tidal asymmetry (section 3.3).
- The neap-spring tidal variation of the asymmetry of the vertical tide (section 3.4).
- The relation between the morphology (hypsometry) of the estuary and the tidal asymmetry (section 3.5).

Most of the analyses presented in this chapter focus on the tidal time scale as defined in section 2.1. This implies that in most cases the morphology is considered time invariant.

Before focusing on the aforementioned aspects, the main hydrodynamic and morphologic characteristics of the estuary are summarised in section 3.2. For a more complete overview of the evolution of the estuary, the reader is referred to Van den Berg et. al. (1996).

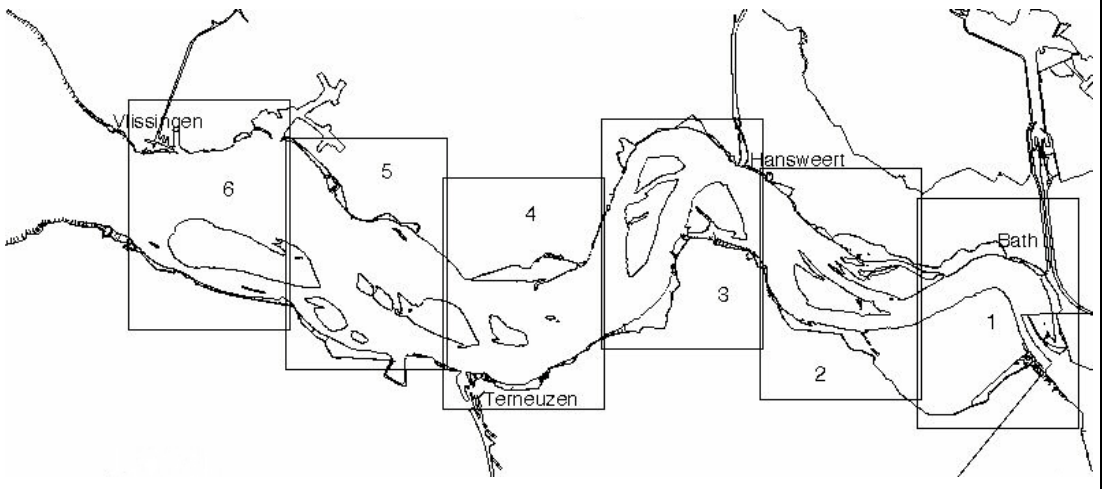

Fig.3.1 Western Scheldt and the six echo-sounding areas.

3.2 Description Western Scheldt

3.2.1 Hydrodynamics

The Schelde estuary is a meso-tidal estuary. Water level observations along the estuary show an increase in mean tidal range between Vlissingen and Antwerpen (78km further upstream) from 4m to 5.2m. This amplification of the tidal range is due to landward convergence, shoaling and partial reflections. Landward of Antwerpen the tidal range decreases as a result of frictional damping. The vertical tide exhibits an asymmetry: the duration of falling tide exceeds that of the rising tide. This duration asymmetry increases in landward direction and with the tidal range (see Table 3.1).

Tidal condition	Vlissingen (mouth)	Antwerpen (78 km further upstream)
neap tide	25	54
mean tide	30	100
spring tide	36	140

Table 3.1 Duration difference (minutes) between tidal fall and rise at Vlissingen and Antwerpen during the neap-spring tidal cycle (data based on Claessens and Meyvis, 1994).

Observations and model computations reveal a phase difference between the horizontal and vertical tide of 2.5 to 3 hours (e.g. Jeuken, 1998, in prep.). Hence the tidal wave is neither completely progressive nor standing. Maximum flood flow occurs about 1.5 hours before the end of the flood (slack water), whereas maximum ebb flow occurs three to four hours after slack water before the ebb (hereafter referred to as SBE). The maximum depth-averaged current velocities in the channels of the estuary are typically of the order of 1-1.5m/s. These velocities in combination with the medium fine sediments (200-300 μm) at the bed induce a sediment transport that is dominated by suspended load transport.

The marine part of the estuary, the Western Scheldt, is well-mixed. The mean river outflow is about $120 m^3/s$, or $2.5*10^6 m^3$ per ebb or flood period. This is less than one percent of the tidal volume of $1*10^9 m^3/s$ at the seaward boundary (Vlissingen).

3.2.2 Morphology

The estuary has a funnel-shaped geometry and a well developed system of channels and shoals. The larger main channels in the estuary display a repetitive pattern, referred to as estuarine sections (Jeuken in prep.). Each of these consists of a meandering ebb channel and a straight flood channel. In most sections these channels are separated by inter-tidal shoals and linked by smaller connecting channels. As discussed in Chapter 2 tidal asymmetry strongly depends on the hypsometric properties of the channel and shoal system in an estuary.

For the evaluation of the relationship between the asymmetry of the horizontal and vertical tide (section 3.3), as well as the relationship between morphology and the asymmetry of the vertical tide (section 3.5), it necessary to quantify the large-scale hypsometric properties of

the channel and shoal system. Therefore the hyposmetric curves given by Mol et.al. (1997) for six (echo-sounding) areas covering the Western-scheldt both in 1996 and in 1955 were analysed by means of curve fitting. From this analysis it appears that the water volume below a vertical reference level z can be described by the following function

$$V = C(d+z)^{\alpha} \tag{3.1}$$

in which

V	=	wet volume between the bed and the plane z=constant(Million m^3)
z	=	vertical coordinate (m)
C	=	coefficient (not dimensionless)
d	=	maximum depth (m) below reference level (NAP)
α	=	coefficient

This equation can also be written as

$$V = Cd^{\alpha}\left(1+\frac{z}{d}\right)^{\alpha}$$

The coefficients Cd^{α} and α for the six parts are given in the following table. The coefficient Cd^{α} is the volume at the reference level (Dutch ordnance level NAP).

Table 3.2 Parameters characterising the hypsometry

	1955			1996		
Vak	d(m)	α	Cd^{α}	d(m)	α	Cd^{α}
1	20	2.70	131.9	20	1.94	182.5
2	20	2.57	254.8	20	2.16	270.0
3	30	2.47	503.0	30	2.67	472.8
4	40	3.59	441.3	40	3.59	441.3
5	50	3.99	670.7	50	4.42	691.3
6	40	3.43	631.2	40	3.43	631.2

The fit appears to be very good (Fig.3.2). The uniformity of the curves for the various parts is intriguing. This uniformity might be related to/ explained by the regular and repetitive pattern of channels and shoals, i.e. the occurrence of the estuarine sections.

The storage area at a certain level is

$$F = \frac{\partial V}{\partial z} = \alpha C(d+z)^{\alpha-1} \tag{3.2}$$

The averaged cross-sectional area is

$$A = \frac{V}{L} = \frac{C}{L}(d+z)^{\alpha} \tag{3.3}$$

Where L is defined as the length of the considered sections. The obtained relationships for the hypsometric curves will be used and further elaborated in sections 3.3 and 3.5.

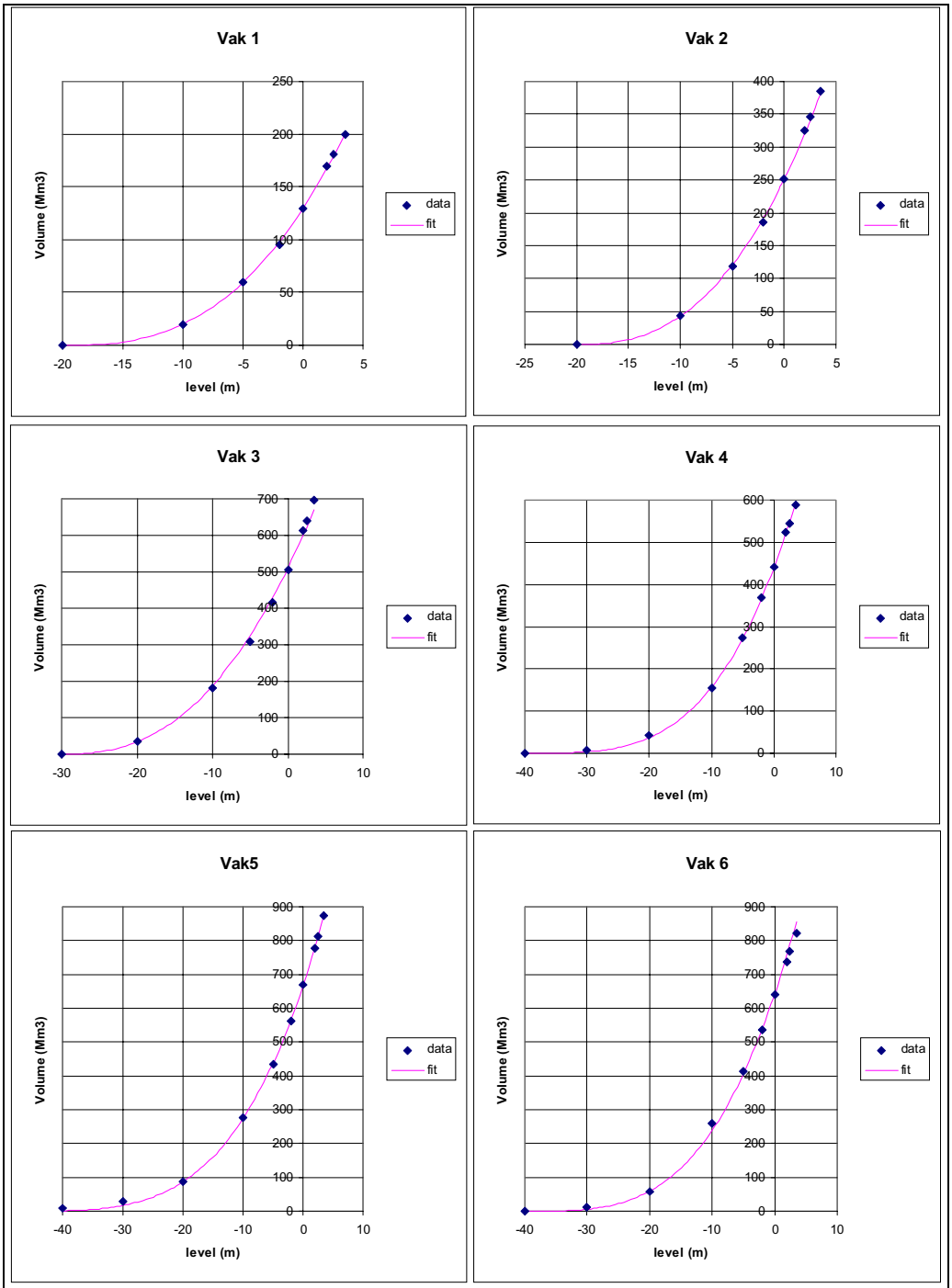

Fig. 3.2a Hypsometry in 1955

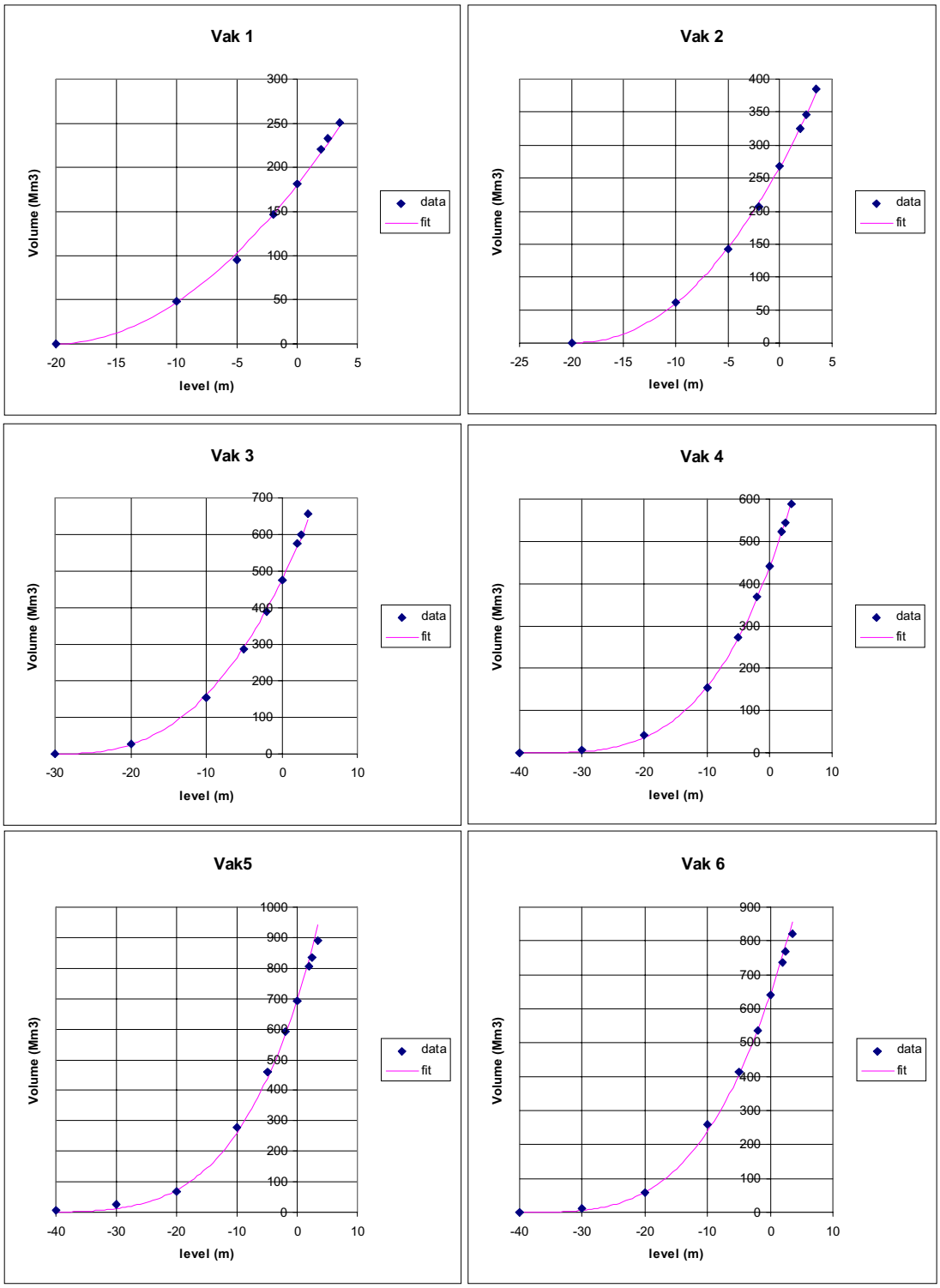

Fig.3.2b Hypsometry in 1996.

3.3 Mechanisms generating tidal asymmetry

3.3.1 Residual flows

Various non-linear interactions of the M_2 tidal component with itself and with other fundamental constituents result in the local generation of residual flows, overtides (M_4, M_6 etc.) and compound tides (e.g. MS_4, see Ch. 2. , Table 2.1). In addition, more global mechanisms may give rise to asymmetries and residual flows.

As discussed in chapter 2 three mechanisms may induce residual flows (rectification), viz.:

- Bathymetry (topography) related circulations that are largely caused by non-linear friction. An extreme form of topography induced residual flow is the general flood-dominated residual flow in inter-tidal areas.
- Horizontal geometry induced residual flows. These mainly originate from inertial effects and non-linear advection.
- Coriolis induced residual currents.

Both the results of 2D-numerical flow modelling and current observations reveal various residual circulations in the estuary that largely coincide with the pattern of ebb and flood channels (Van de Male, 1993, Jeuken, 1996, 1998, in prep.,). If ebb channels are defined as channels that have a bar at their seaward end, whereas the flood channels tend to exhibit a relatively shallower bar at their landward end, ebb-dominated residual flows occur in the ebb channels whereas flood-dominated residual currents prevail in the flood channels. This (qualitative) relationship between channel morphology and the direction of residual flow suggests that these circulations are bathymetry-induced: they originate from interactions between the channel geometry and the residual flow. Furthermore it appears that the direction of the residual flow (ebb or flood) largely determines the asymmetry of maximum flow, i.e. the difference between maximum ebb and flood velocities in a channel.

Ebb and flood-dominated residual flows within straight stretches of an individual channel can hardly be identified from the results of 2D flow simulations. This suggests that the Coriolis effect is of minor importance in the generation of the residual flows. The same seems to apply to the horizontal geometry induced circulations.

The above-described phenomenom of bathymetry induced circulations is illustrated on the basis of long-term (4 weeks) current observations at two locations in the seaward (western) part of the estuary. One current meter was deployed in the central part of the main flood channel ‘Everingen’, whereas a second one was situated in the main ebb channel ‘Pas van Terneuzen’. From short-term observations (1 tide) of the vertical velocity profile it appeared that the velocity profiles near these current meter locations exhibit a more or less logarithmic shape. Based on this obervation and the simultaneously measured water level at Terneuzen the observed current velocities (at z/h=0.4) were converted to depth-averaged velocities (by applying a logarithmic current profile). The residual currents at the two stations were obtained by removing the tidal variation in the time-series. This was done by applying the low pass Godin-filter (1972). This filter eliminates the M_2 and S_2 components entirely and all other components with periods shorter than 30 hours for more than 99 percent. Figure 3.3

displays the residual depth-averaged velocities at the two stations. The long-term mean residual current at the location in the flood channel is flood-dominated and approximates 0.1m/s. At the location in the ebb channel an ebb-dominated (negative) residual flow of some 0.17m/s prevails. In addition a pronounced neap-spring tidal modulation of the residual currents can be observed: during spring tide (e.g. day 265) they are about twice as large as during neap tide (day 272).

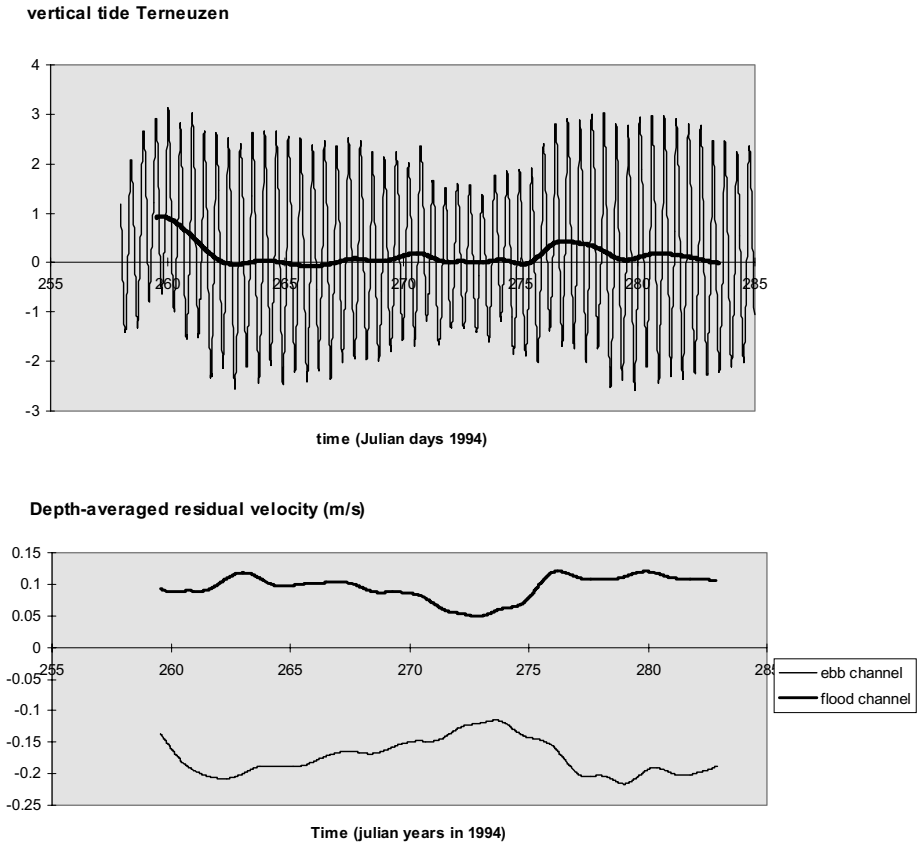

Fig.3.3 Residual water levels and current velocities in the Western part of the estuary measured near Terneuzen in 1994. Panel a) Tidal and residual water level. Panel b) Current velocity in the main ebb and flood channel 'Pas van Terneuzen' and 'Everingen'.

To conclude, the bathymetry induced residual flow appears as a prominent feature in the residual water motion in the estuary. At most locations in the estuary the total cross-sectionally averaged residual velocity is the net (small) effect of a relatively large residual flood flow in the flood channel and an ebb-dominated residual flow in the ebb channel. The intensity (magnitude) of residual circulations induced by the ebb and flood channels exhibits a neap-spring tidal variation.

3.3.2 Relation between asymmetries in vertical and horizontal tide

The integrated continuity equation (2.16) is used to analyse the influence of the hypsometry on the tidal asymmetry by investigating the relation between the vertical tide and the horizontal tide.

The analysis presented here has the following restrictions:

- The analysis does not concern the discharge or flow velocity at a certain location directly, but it concerns the difference of discharges / velocities between two cross-sections.
- The analysis applies to 'a single channel system'. It doesn't include the effect of ebb-dominated and flood-dominated channels within a cross-section.

Despite these restrictions, the analysis gives useful insight into the relation between the asymmetry of the vertical tide and that of the horizontal tide, and especially into the influence of the hypsometry on this relation.

Linear solution

If the variation of storage area F and cross-sectional area A with respect of z is not taken into account, the integrated continuity equation suggests a linear relation between the vertical tide and the horizontal tide. Consider a vertical tide consisting of a semi-diurnal, a quarter-diurnal and a sixth-diurnal component

$$\zeta = a_2 \cos(\omega t) + a_4 \cos(2\omega t - \varphi_4) + a_6 \cos(3\omega t - \varphi_6) \tag{3.4}$$

with the amplitude ratio

$$a_2 : a_4 : a_6 \cong O(1) : O(\delta) : O(\delta) \tag{3.5}$$

Substitution of equation 3.4 into the integrated continuity equation (eq. 2.16) learns that the amplitude ratio of the corresponding discharge components is

$$Q_2 : Q_4 : Q_6 = 1 : 2\frac{a_4}{a_2} : 3\frac{a_6}{a_2} \cong 1 : O(2\delta) : O(3\delta) \tag{3.6}$$

The same ratios apply for the flow velocity

$$u_2 : u_4 : u_6 = 1 : 2\frac{a_4}{a_2} : 3\frac{a_6}{a_2} \cong 1 : O(2\delta) : O(3\delta) \tag{3.7}$$

Non-linear solution

For a area with a length that is small relative to the tidal wave length the integrated continuity equation can be written as

$$\Delta Q = F(\zeta)\frac{\partial \zeta}{\partial t} \tag{3.8}$$

Herein

ΔQ = difference between the discharges at the begin and end of the area,
F = storage area,
ζ = averaged water level in the area.
A = cross-sectional area

If the area can be considered as prismatic, the flow velocity becomes

$$\Delta u = \frac{F(\zeta)}{A(\zeta)}\frac{\partial \zeta}{\partial t} \tag{3.9}$$

Where

Δu = difference between the velocities at the begin and end of the considered area.

These equations show clearly the significance of the hypsometry on the relation between the horizontal and the vertical tide. In order to show how the hypsometry influences the asymmetry in the horizontal tide, the hypsometry of the Western Scheldt as described in section 3.1 is used in combination with a vertical tide consisting of a semi-, a quarter- and a sixth-diurnal component (eq. 3.4).Further it is assumed that

$$\frac{a_4}{a_2} = O(\delta), \quad \frac{a_6}{a_2} = O(\delta) \text{ and } \frac{a_2}{d} = O(\delta) \quad \text{with} \quad \delta << 1 \tag{3.11}$$

The condition $\delta<<1$, say 0.1, implies deep channels. For the Western Scheldt this is a reasonable assumption. Therefore the first order Taylor series will be used for F and A for the analysis:

$$F(\zeta) \approx F(0) + \zeta \left.\frac{\partial F}{\partial z}\right|_{z=0} = F(0)\left[1 + (\alpha - 1)\frac{\zeta}{d}\right] \tag{3.12}$$

and similarly

$$\frac{F(\zeta)}{A(\zeta)} = \frac{\alpha L}{d+\zeta} \approx \frac{\alpha L}{d}\left(1 - \frac{\zeta}{d}\right) \tag{3.13}$$

It is noted that the truncated Taylor series (eq. 3.11) only works for a small ζ.

Substituting (3.11) and (3.12) into (3.8) and (3.9) yields

$$\Delta Q = -F(0)a_2\omega\left[\sin(\omega t)+2\frac{a_4}{a_2}\sin(2\omega t-\varphi_4)+3\frac{a_6}{a_2}\sin(3\omega t-\varphi_6)\right]+ \\ -F(0)(\alpha-1)a_2\omega\frac{a_2}{d}\sin(\omega t)\cos(\omega t)+\text{higher order terms in }\delta \tag{3.14}$$

$$\Delta u = -\frac{\alpha L}{d}a_2\omega\left[\sin(\omega t)+2\frac{a_4}{a_2}\sin(2\omega t-\varphi_4)+3\frac{a_6}{a_2}\sin(3\omega t-\varphi_6)\right]+ \\ -\frac{\alpha L}{d}a_2\omega\frac{a_2}{d}\sin(\omega t)\cos(\omega t)+\text{higher order terms} \tag{3.15}$$

The leading (first order) term due to the non-linear interaction under influence of the hypsometry is thus a quarter-diurnal one. The summation of the two quarter-diurnal terms in equation 3.15 (neglecting all the second order terms) results in the following expressions for the amplitude ratios of the discharges *q* and velocities *v*

$$\frac{\Delta q_4}{\Delta q_2} = 2\frac{a_4}{a_2}\sqrt{1+\frac{1}{2}(\alpha-1)\frac{a_2}{d}\frac{a_2}{a_4}\cos\varphi_4+\frac{(\alpha-1)^2}{16}\left(\frac{a_2}{d}\frac{a_2}{a_4}\right)^2} \tag{3.16}$$

$$\frac{\Delta v_4}{\Delta v_2} = 2\frac{a_4}{a_2}\sqrt{1-\frac{1}{2}\frac{a_2}{d}\frac{a_2}{a_4}\cos\varphi_4+\frac{1}{16}\left(\frac{a_2}{d}\frac{a_2}{a_4}\right)^2} \tag{3.17}$$

$$\frac{\Delta q_6}{\Delta q_2} = \frac{\Delta v_6}{\Delta v_2} = 3\frac{a_6}{a_2} \tag{3.18}$$

where

$\Delta q_\#$	=	difference in the discharge between the begin and end of the considered section induced by the #-diurnal component.
$\Delta u_\#$	=	difference in the velocity between the begin and end of the section induced by the #-diurnal component.
φ_4	=	the phase difference between the quarter-diurnal and semi-diurnal tide.
d	=	the maximum depth in the considered area.
$a_\#$	=	the amplitude of the #-diurnal component of the vertical tide.

For the Western Scheldt the phase difference between the quarter-diurnal tide and the sem-diurnal tide, φ_4, is small. This means that the (quarter-diurnal) asymmetry in the discharge is enhanced by the hypsometry whereas the asymmetry in the flow velocity is weakened by the hypsometry. This explains why, for instance, a flood-dominant duration asymmetry (shorter rise) of the vertical tide is not necessarily accompanied by a flood dominant magnitude asymmetry (larger flood velocity) of the horizontal tide.

In summary:

- The asymmetry of the horizontal tide, discharge as well as flow velocity, is stronger than that of the vertical tide. This is mainly due to the fact that the frequency of the overtides and the compound tides causing the tidal asymmetry have a higher frequency.
- The quarter-diurnal component of the discharge is larger than the linear solution suggests.
- The quarter-diurnal component of the flow velocity is smaller than according to the linear solution, but still larger than a_4/a_2.
- The sixth-diurnal components of the flow velocity and of the discharge are both larger than the linear solution suggests, but the difference is of higher order δ.

3.3.3 Asymmetry of observed horizontal tide

Sufficient information on the asymmetry of the vertical tide in the Western Scheldt estuary is available, as an extensive data set exists for the tidal constituents at various stations. However, for the tidal constituents of the horizontal tide the information is scarce, simply because the derivation of tidal constituents requires long-term observations which are much more difficult to obtain for the horizontal tide. Long-term discharge observations are often to expensive. In practice impossible only some long-term single-point velocity records are available. Here the previously-described (section 3.3.1) depth-averaged flow velocity records were harmonically analysed to investigate the characteristics of the asymmetry of the horizontal tide at two locations in the western part of the Western Scheldt.

Since the flow velocity is a vector, each tidal constituents of the velocity is represented by an ellipse. In general, it is no longer possible to characterise the asymmetry by a amplitude ratio and a relative phase difference. Each constituent is characterised by the direction of the principal axis of the ellipse, the amplitudes along the two axes and the corresponding phase. So there are four independent parameters instead of two. The question arises how the asymmetry should be characterised now. Note that the analysis of Van de Kreeke and Robaczewska (1993) is in fact only for 1D cases. One may also wonder if it is possible and/or necessary to extend the theory to general 2D case.

The ellipses of M_2 and its overtides for the two stations are shown in Fig.3.4. For the station in the ebb channel the following observations are made:

- The principal directions of M_2, M_4 and M_6 are not the same. The principal direction of M4 is almost perpendicular to that of M_2. The M_6 has a direction in between the two.
- The magnitude of the M6 constituent is larger than that of M_4 .which is very small for this station.

That the principal direction of the M_4 tide is almost perpendicular to that of the M_2 is probably caused by secondary flow due to curvature. The secondary flow due to curvature is perpendicular to the longitudinal flow and its magnitude is proportional to the absolute value of the velocity magnitude in the longitudinal direction. The frequency of the variation of the secondary flow is exactly two times that of the main flow. This means that in a estuary where the tide is dominated by the M_2 component, M_4 will be the dominating component of the secondary flow due to curvature. The station under consideration is indeed located in a bend.

For the station in the flood channel the following observations are made:

- The principal directions of M_2, M_4 and M_6 are not the same but the differences are much smaller than in the ebb channel.
- The magnitude of the M_4 component is much larger than in the ebb channel.

The tidal constituents along the principal direction of M_2 at the two stations are given in Table 3.3. It is remarkable that the MS_4 plays an important role in the quarter-diurnal tide, and the $2MS_6$ is even the largest sixth-diurnal component at both stations. The latter points at a strong-neap spring tidal variation of the quarter-diurnal and sixth-diurnal asymmetry. The consequences for the sediment transport and morphology are not known yet. This requires additional research.

Tabel 3.3 Tidal constituents of the velocity along the principal direction of M2 tide

Component		Ebb channel		Flood channel	
		Amplitude	Phase	Amplitude	Phase
	mean	-0.162		0.088922	
diurnal	O1	0.026	142.9	0.025	131.9
	K1	0.021	20.7	0.022	320.1
	P1	0.007	16.5	0.007	315.9
semi-diurnal	M2	0.739	0.9	0.721	347.1
	S2	0.205	61.2	0.184	47.4
	K2	0.059	61.2	0.053	47.4
	N2	0.135	355.8	0.124	349.1
quarter-diurnal	MN4	0.01	146.8	0.043	88.2
	M4	0.018	32.1	0.122	87.7
	MS4	0.031	125.2	0.102	134.9
sixth-diurnal	2MN6	0.033	158.1	0.048	121.2
	M6	0.065	155.4	0.08	122.5
	2MS6	0.093	202.3	0.102	165.7

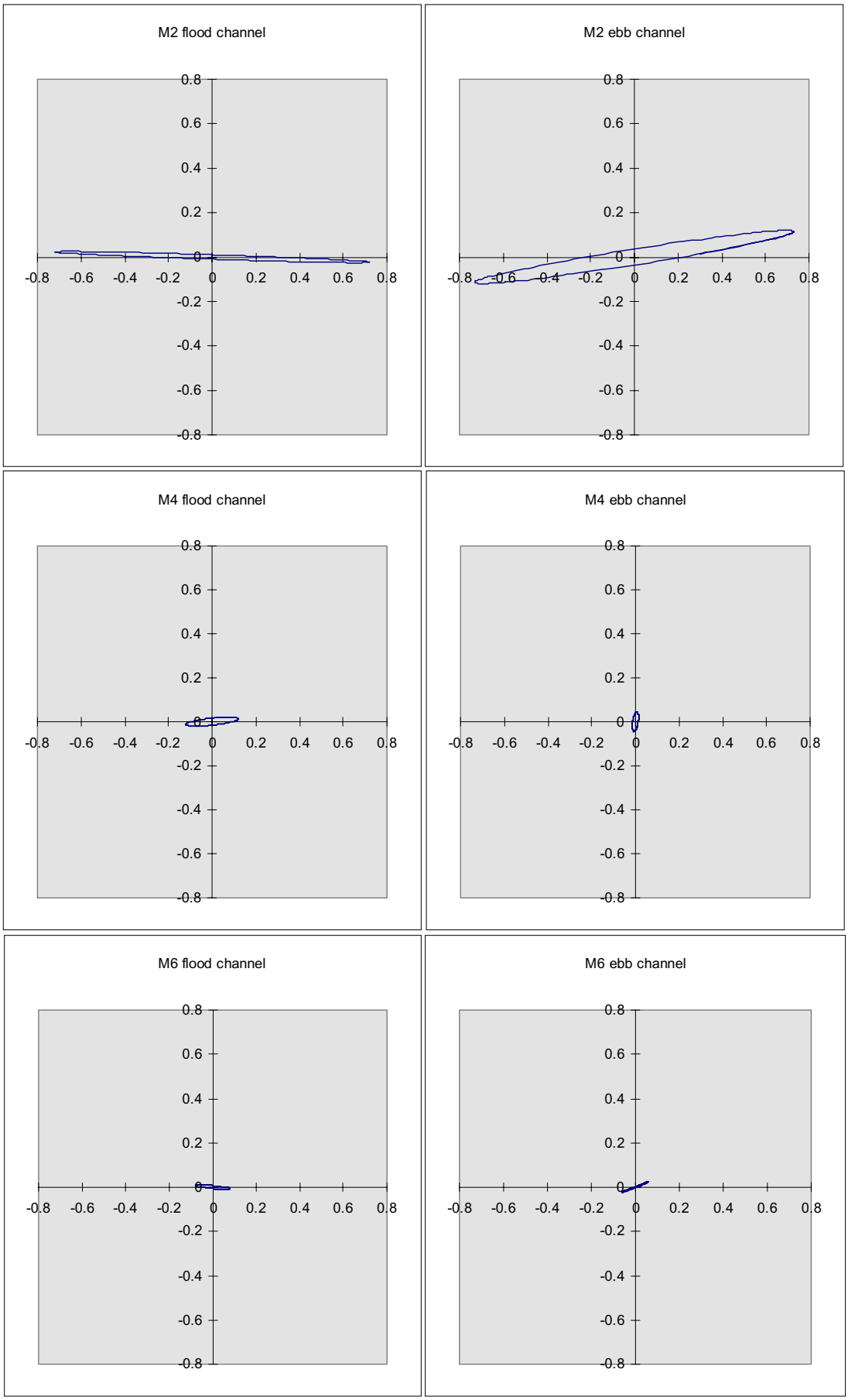

Fig3.4 Ellipses of M2, M4 and M6 tide at two considered current meter stations.

3.4 Temporal variation of the asymmetry of the vertical tide

The literature survey (Chapter 2) has shown that both indicating parameters (amplitude ratio and phase difference) for tidal asymmetry are time-varying. This applies to the predicted as well as the measured tide, although it is not clear if the characteristics of the variations are the same. The tidal asymmetry exhibits an important variation over the spring-neap cycle.

Predicting the tide at Vlissingen with 9 tidal constituents shows some typical characteristics of the variations of the two parameters in the spring-neap cycle. The question arises whether this typical temporal variation pattern of the tidal asymmetry over a spring-neap cycle is due to physical causes, or simply to the presentation of tide-signal in the frequency domain. The answer to this question is of significant theoretical and/or practical importance. If physical causes are behind the variation pattern it is important to know which processes and/or mechanisms give rise to it. Also if the variation pattern is caused by the presentation of the tide in the frequency domain, it is of great importance to the morphodynamic modelling practise. Most morphodynamic models work with the so called morphological tide, which is chosen somewhere between the mean and the spring tide. The predicted astronomical tide is often used and it is usually made periodic by representing it by a Fourier series.

To obtain the answer of the question, one only needs to investigate whether the observed tide (in the time domain) exhibits the same variation pattern of the tidal asymmetry as the predicted astronomic tide. If this is the case then it can be concluded that the variation pattern is due to physical reasons. Otherwise it is probably caused by the presentation of tide in the frequency domain.

The temporal variation of the asymmetry of the predicted vertical tide at Vlissingen has already been analysed in Chapter 2. The recorded water level at Vlissingen of 45 lunar days is used here to analyse the asymmetry of the predicted tide. The semi-, quarter-, and sixth-diurnal components at each lunar day are determined by carrying out a Fourier analysis. The results are shown in the Fig.3.5-Fig.3.9. The following observations / conclusions are made:

- The amplitude ratios a_4/a_2 and a_6/a_2 increases with the increase of the amplitude of the semi-diurnal tide (Fig. 3.6, 3.8). The asymmetry of the tide is thus stronger at spring tide than at neap tide. The averaged value of the ratios are about a_{M4}/a_{M2} and a_{M6}/a_{M2} respectively. This agrees with the conclusion derived from the analysis of the predicted tide.
- Like in the results based on the tidal constituents there is not a simple relation between a_2 and a_4/a_2 but there is a large scatter (Fig 3.8). However, the conclusion that the ratio is larger during the period from spring to neap than from neap to spring does not apply to the observed tide.
- The relative phase difference between the quarter-diurnal and semi-diurnal tide shows a scatter around the value $2\varphi_{M2}-\varphi_{M4}$ (Fig. 3.7 and 3.9). The scatter is larger at neap tide than at spring tide. So far it agrees with the results based on the tidal constituents. However, the scatter here is a random one rather than the ordered scatter in the picture based on the tidal constituents (i.e. the predicted tide). The conclusion that the phase difference is larger in the period from spring to neap than from neap to spring is not supported by the observations. The same applies to the relative phase difference between the sixth-diurnal and the semi-diurnal tide (Fig 3.7 and 3.9).

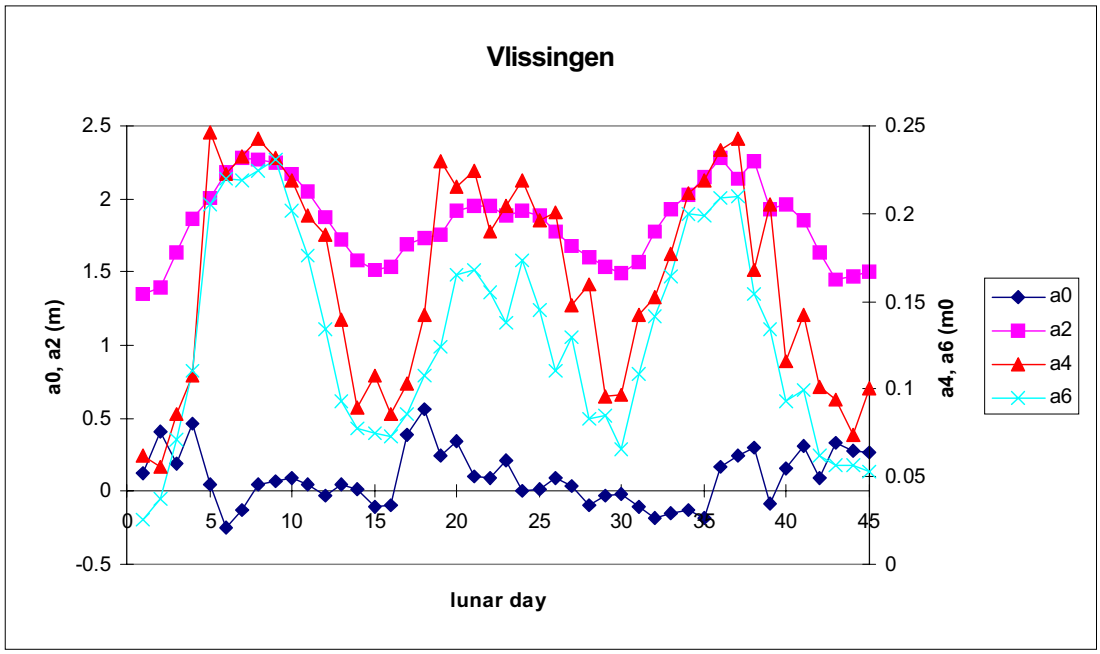

Fig.3.5 Variation of mean level and amplitudes of semi-, quarter- and sixth-diurnal tides

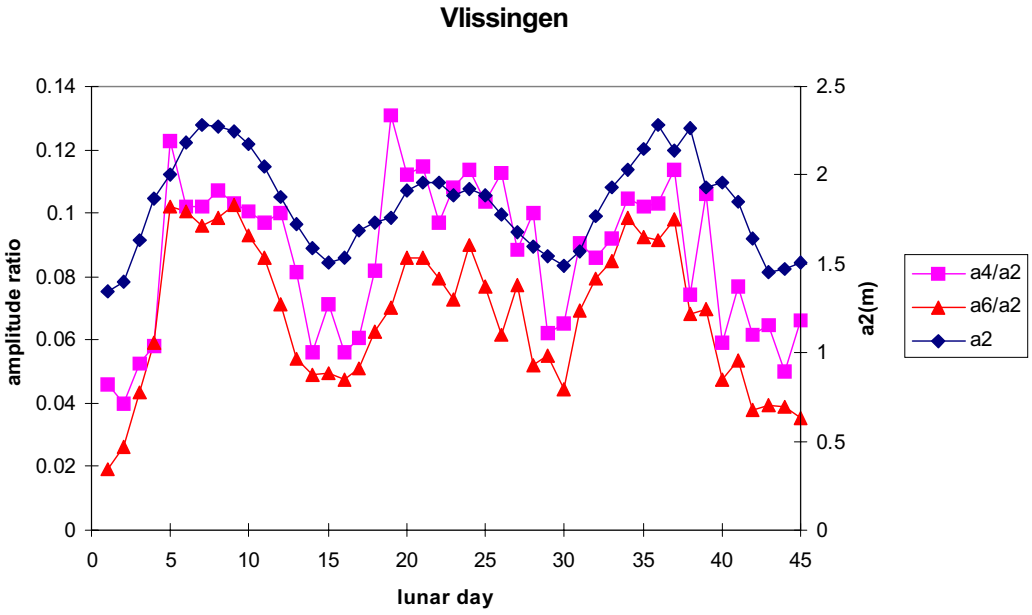

Fig.3.6 Variation of the amplitude ratios

Error! Not a valid embedded object.

Fig.3.7 Variation of the relative phase difference

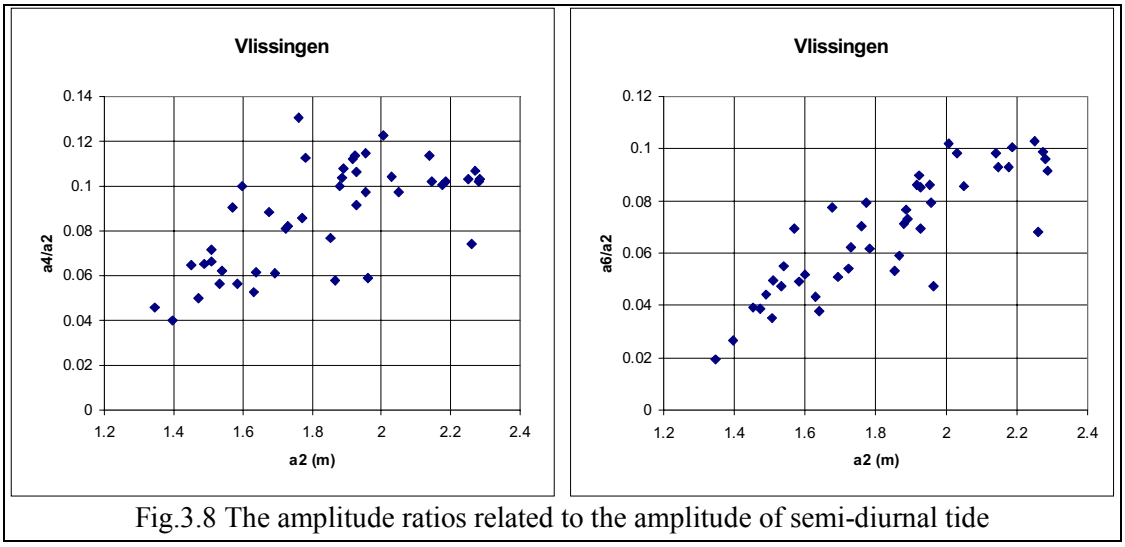

Fig.3.8 The amplitude ratios related to the amplitude of semi-diurnal tide

This leads to the conclusion that some of the variation characteristics of the tidal asymmetry are the same for predicted and the observed tide, whereas others are not. That the tidal asymmetry is stronger at spring tide than at neap tide is the most important common characteristic. The physical reason behind this is apparently that the non-linear interactions as described in Chapter 2 are more important during spring tide than during neap tide. The most important difference between the predicted and observed tides is the ordered scatter in the predicted tide versus the random scatter in the observed tide. However, this difference may be due to the restricted number of tidal constituents used to predict the tide. This would not be a surprising conclusion considering the fact that that with only two base constituents (in total six constituents) the relation is a closed line whereas with three base constituents (in total nine constituents) it already becomes a chaotic picture.

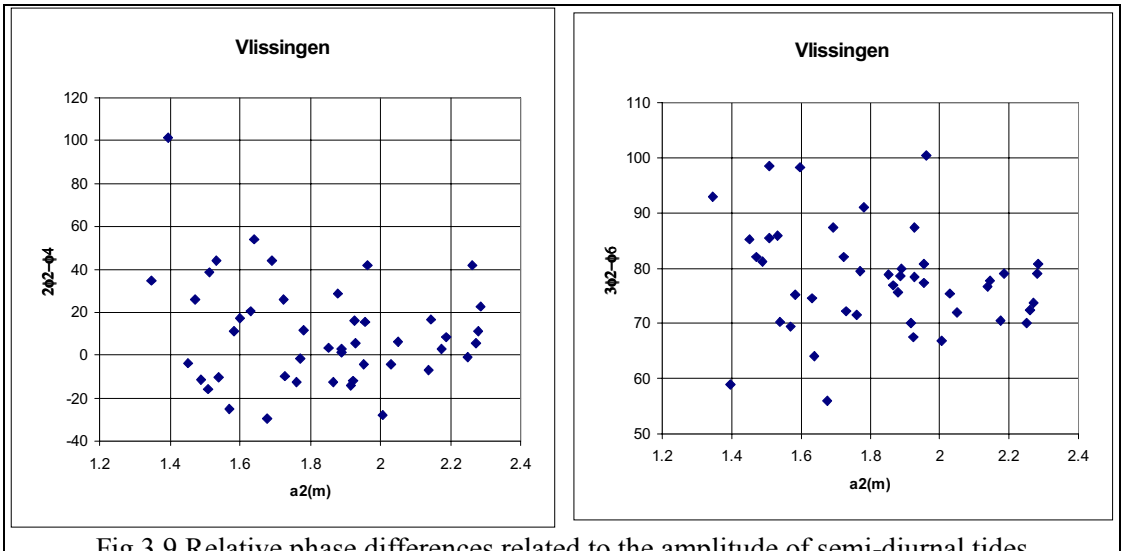

Fig.3.9 Relative phase differences related to the amplitude of semi-diurnal tides

In the morphodynamic modelling of coastal systems a so called morphological tide is often used to represent the tidal forcing. There are various methods to determine the morphological tide. One of them involves the selection of a period within a spring-neap cycle and making the tide periodic. Because of the non-linear relation between the sediment

transport and the flow velocity it is generally suggested that the morphological tide should be slightly larger than the mean tide . The underlying tidal data can originate from tidal prediction or measurements. Note that the tide at the model boundary is often generated by running a larger model with the astronomical tide at the open boundaries. Here too the 'data' is in fact based on a tidal prediction. From the present analysis it is clear that this method of determining the morphological tide, whether prediction or observation-based is susceptible to large errors in the tidal asymmetry due to the overtides:

- Picking an arbitrary time-interval means choosing a point in the wide scatter of Fig. 3.8 and Fig.3.9. This means that the amplitude ratio as well as the relative phase difference can be far from the long-term average.
- When using observed data, it is not well known which sign the error will have.
- When using a predicted tide the error will depend on whether the interval is chosen in the half-cycle from from neap to spring or from spring to neap, it also depends on the number of tidal constituents used.

For the quarter-diurnal and the sixth-diurnal components of the morphological tide it is probably better to simply use the theoretical value based on M_2, M_4 and M_6, rather than the results of the Fourier analysis for an arbitrarily selected time-interval.

3.5 Relation between tidal asymmetry and morphology

A first discussion on the relation between the morphological development and the development of the tidal asymmetry is given by Gerritsen et al (1999). It appears that the results in the literature, e.g. those of Speer et al (1991), are qualitatively applicable to the Western Scheldt, especially when the change of the tidal asymmetry is considered.

In the present sectiom, the influence of morphological characteristics on the tidal asymmetry will be discussed in further detail. Various geometry parameters have been used for characterising tidal asymmetry in estuaries. All of these parameters suggest that the intertidal area and the depth of the estuary are important. Estuaries with a relatively large intertidal areas tend to be ebb-dominant and relatively shallow estuaries tend to be flood-dominant. The discussion here will focus on the following questions:

- Which parameters are the most appropriate for characterising the geometry of the Western Scheldt from the perspective of tidaltidal asymmetry?
- Are there parameters, in addition to the ones already mentioned in the literature, that are important for the tidal asymmetry in the Western Scheldt?

3.5.1 Tidal asymmetry with respect to quarter-diurnal tide

The two parameters indicating tidal asymmetry for the four stations in the Western Scheldt (Vlissingen, Terneuzen, Hansweert and Bath) in the period 1971-1997 are given in Fig.3.10. A discussion of the development shown by this figure is given by Gerritsen et al (1999). Here it is noted that the tidal asymmetry of the vertical tide in the different parts of the estuary is not the same.

The tidal asymmetry in an estuary is influenced by the asymmetry of the tide at the seaward boundary of the system (e.g. Van der Spek, 1994). Similarly, it is likely that the tidal asymmetry at a certain station is interrelated with the tidal asymmetry in the downstream

(seaward) located area. Based in this presumption it is hypothesised that *the change of the tidal asymmetry in a certain part of the estuary, rather than the tidal asymmetry itself, should be related to the morphological characteristics and developments of this part of the estuary.* This hypothesis will be used as guideline in the analysis below.

The change of the tidal asymmetry between two stations is represented by the ratio of the two amplitude ratios and the difference between the relative phase differences. The two parameters are thus defined as

$$\left(\frac{a_4}{a_2}\right)_{station\,2} \Big/ \left(\frac{a_4}{a_2}\right)_{station\,1} \quad \text{and} \quad \left(2\varphi_2 - \varphi_4\right)_{station\,2} - \left(2\varphi_2 - \varphi_4\right)_{station\,1} \tag{3.19}$$

These two parameters for the sections Terneuzen-Vlissingen, Hansweert-Terneuzen and Bath-Hansweert are shown in Fig.3.11 The trend in the historical development is better visible than in Fig.3.10.

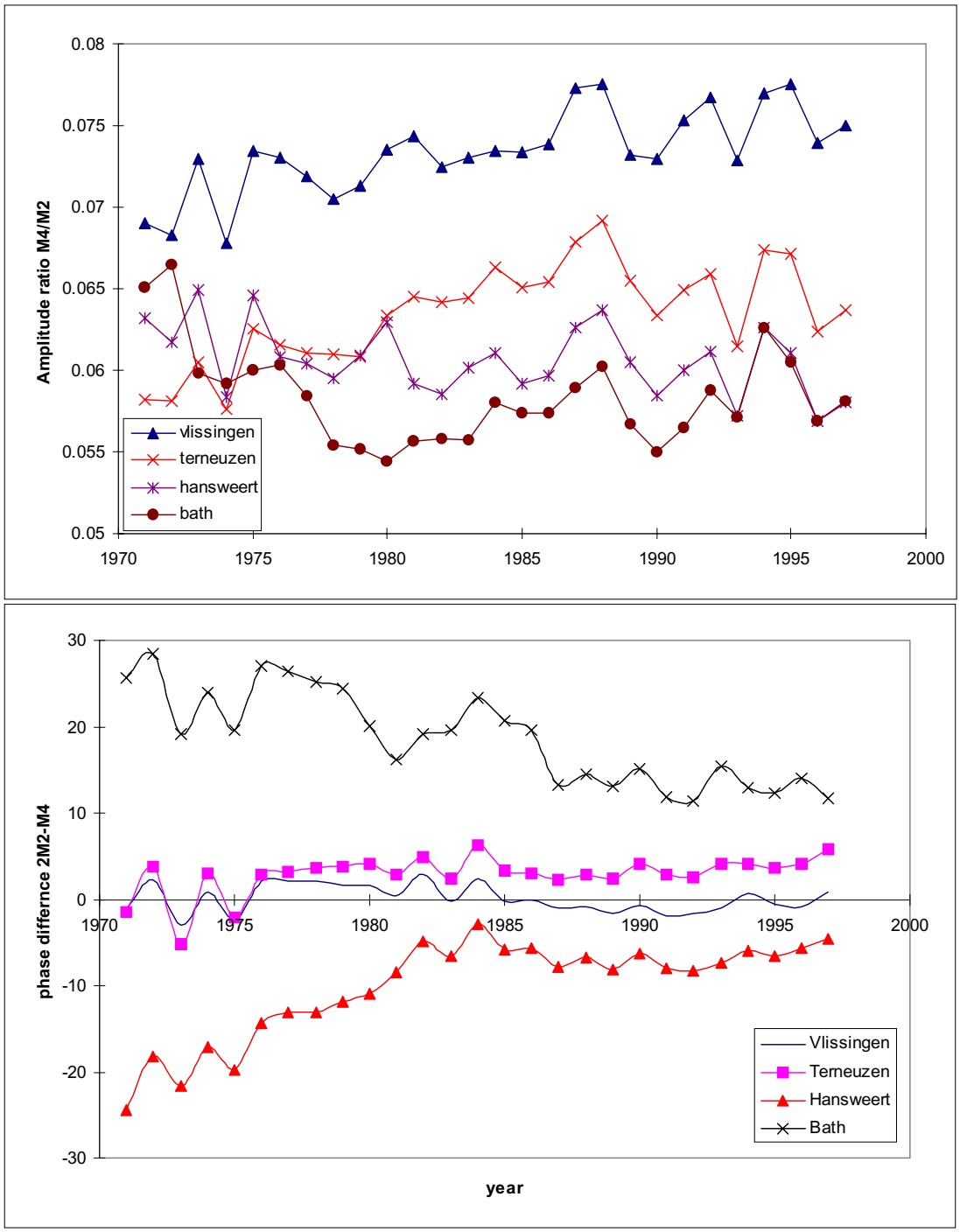

Fig3.10 Development of the amplitude ratio and phase difference between the M_2 and M_4 tide.

From figure 3.11 shows the following features regarding the asymmetry of the vertical tide in the three regions of the estuary:

- In the eastern part, between Hansweert and Bath (Vak 1 and 2, Fig. 3.1), the tide is flood dominant. This is indicated by the positive value of the phase-difference parameter Bath-Hansweert (upper panel). The decrease of this parameter between 1971 and 1980, points at a reduction of this flood dominance in time. The amplitude ratio parameter initially decreased and is increasing again since about 1980.

- The central part of the estuary, between Terneuzen and Hansweert (Vak 3 and 4), is ebb-dominant. The ebb-dominance in this area decreased between 1971 and 1985.
- In the western part of the estuary, between Vlissingen and Terneuzen (Vak 5 and 6), the asymmetry of the vertical tide gradually altered from neutral to slightly flood-dominant during the period 1971-1997.

In the following section it will be investigated if this observed development of the tidal asymmetry can be related to the large-scale morphologic (hypsometric) evolution of the channel and shoal system and the net sediment transport directions derived from sand budget studies.

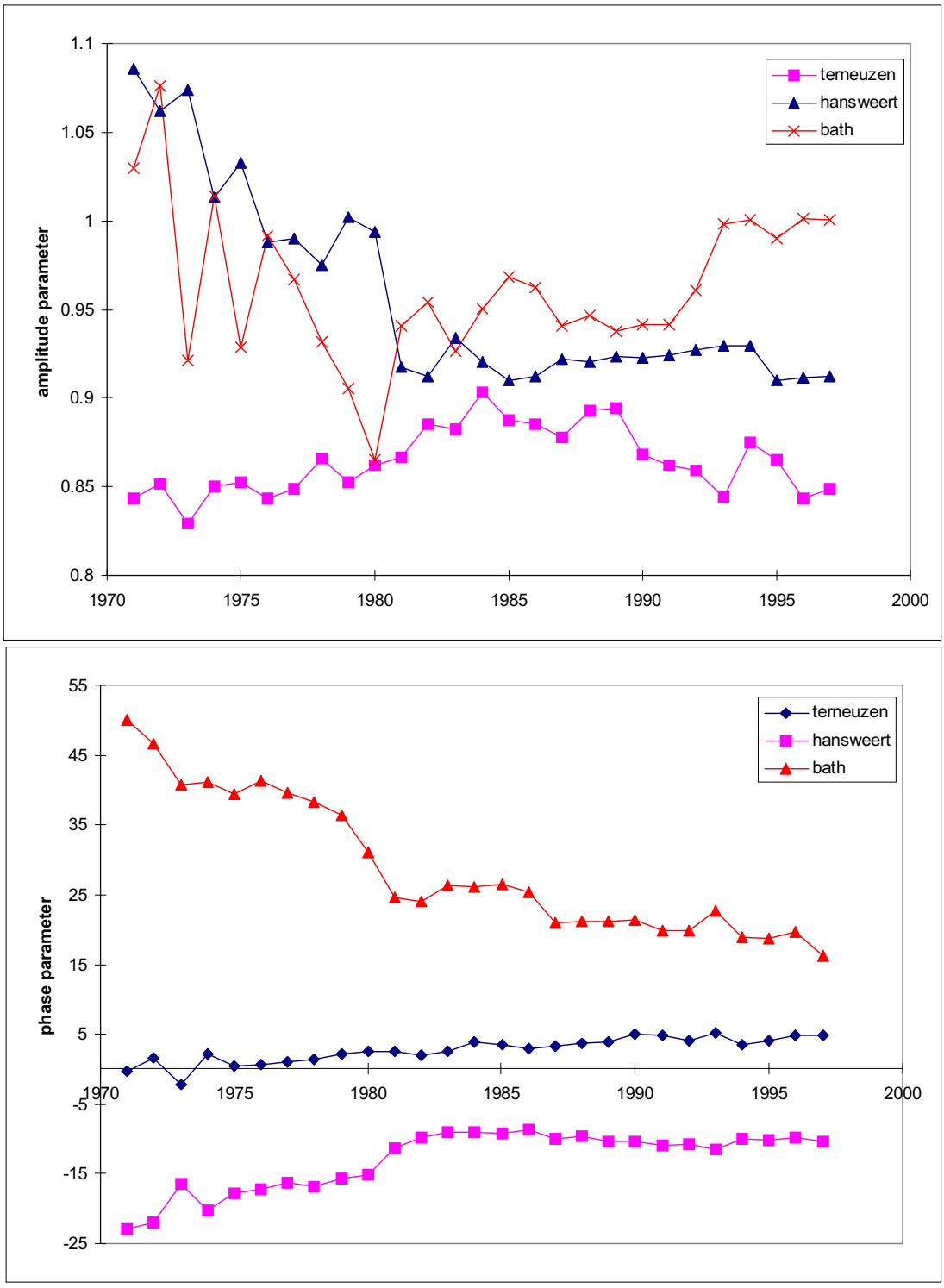

Fig.3.11 Development of the relative amplitude and phase parameters (eq. 3.18). Relative refers to the changes with respect to the seaward located water level station, i.eTerneuzen versus Vlissingen, Hansweert versus Terneuzen and Bath versus Hansweert.

3.5.2 Morphological characteristics and their changes

Using the information of the hypsometry as described in section 3.2 it is possible to derive the morphological parameters used by e.g. Speer et al (1991).

For V_s, the volume of water stored on tidal flat between high and low water, we have

$$V_s = V(a) - V(-a) - 2F(-a)a \tag{3.20}$$

For the channel volume under mean sea level

$$V_c = V(-a) + aF(-a) \tag{3.21}$$

The mean channel depth is

$$h = \frac{V_c}{F(-a)} = \frac{V(-a)}{F(-a)} + a \tag{3.22}$$

Substituting Eq.(3.1) voor V and Eq.(3.2) voor F yields the two indicating parameters as defined by Speer et al (1991):

$$\frac{a}{h} = \frac{\alpha \frac{a}{d}}{1 + (\alpha - 1)\frac{a}{d}} \tag{3.23}$$

$$\frac{V_s}{V_c} = \frac{\left(1 + \frac{a}{d}\right)^{\alpha}}{\left(1 - \frac{a}{d}\right)^{\alpha} + \frac{a}{d}\left(1 - \frac{a}{d}\right)^{\alpha - 1}} - 1 - \frac{\alpha \frac{a}{d}}{1 + (\alpha - 1)\frac{a}{d}} \tag{3.24}$$

These two parameters for the six parts (vak, echo-sounding areas) of the estuary in 1955 and 1996 are shown in the left panel of Fig.3.12. In the right panel the flood- and ebb-dominance of the vertical tide in the six areas is indicated. The latter information is obtained from figure 3.11 (see previous) section. For the morphologic situation of 1955 the tidal asymmetry in 1971 is indicated since information of the tidal asymmetry is not available for 1955. This leads to the following observations / conclusions:

- Most flood dominant parts of the estuary have larger values of a/h as well as V_s/V_c. The fact that larger values of a/h correspond with flood-dominance agrees with the conclusions of Speer et al (1991). Qualitatively the results of Speer et al. (1991) are thus applicable to the Western Scheldt. However, the exact separator between ebb-dominance and flood-dominance as shown in Fig.3.12 is not the same as the one found by Speer et al.(1991, see Fig.2.9). This was to be expected, since the Western Scheldt differs very much from the estuaries considered by Friedrichs et al. (1990).

- There is one point in the right panel that deviates from the general trend. It represents the part Vak 5 in 1996. This area is specified as flood-dominant because, according to Fig.3.11,in 1996 the western part (Vak 5 and 6) shows a slight flood-dominance and because Vak 5 has a larger a/h value than Vak 6. In fig.3.12 this point is located in a region where all other points are ebb-dominant . The conclusion is therefore that the theory of Speer et al (1991) does not explain the flood-dominance of the western part of the estuary in 1996.

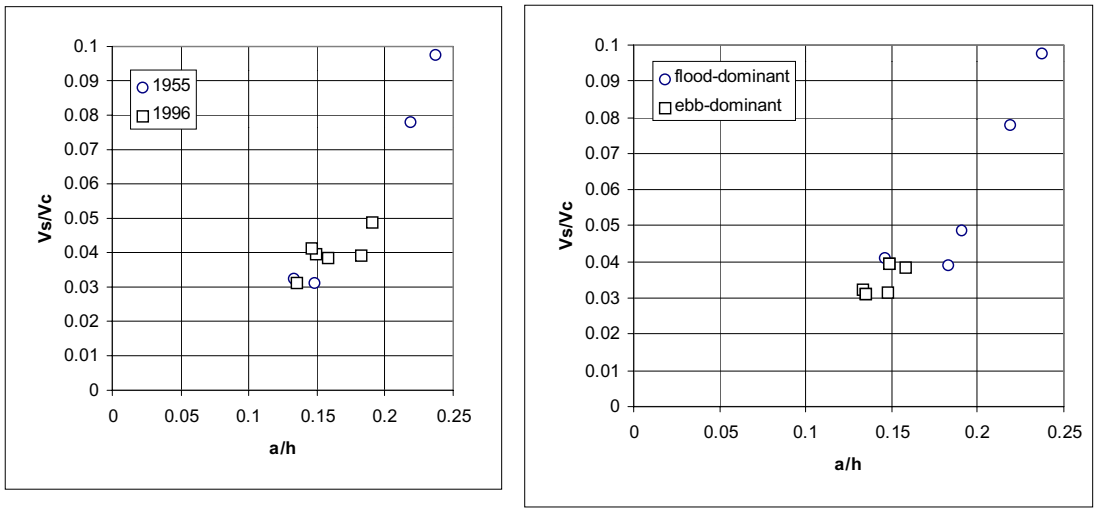

Fig.3.12 The geometric parameters in the six parts of the Western Scheldt in 1955 and 1996 (left) and in relation to the flood ebb-dominance of the vertical tide (right)

The analysis can also be taken one step further by relating the changes of the morphology to the changes of the tidal asymmetry. For this purpose the differences of the two parameters in the two years (1955 and 1996) are related to the change of tidal asymmetry from 1971 to 1997 (Fig.3.13). First the two parameters a/h and V_s/V_c and their changes from 1955 to 1996 are determined for the six parts (the upper panels of Fig.3.13). Then the average changes of the two parameters in the eastern part (averaging Vak 1 and 2), the central part (Vak 3 and 4) and the western part (Vak 5 and 6) are related to the change of the phase difference from 1971 to 1997 as shown in Fig.3.11 (the lower panels of Fig.3.13). The following observations are made:

- Most changes of the two parameters occur in the eastern part of the estuary (Vak 1 and 2).
- The change of the two parameters seem to be related with each other.
- The change of both parameters correlates well with the change of the tidal asymmetry in the corresponding part.

That the changes of the two parameters seem to be related with each other is due to the fact that a/h and V_s/V_c are not independent of each other. This is simply illustrated by the fact that an increase of tidal amplitude, for example, causes an increase in both parameters. In the present case, the changes of both parameters are mainly caused by the changes in the deep channel parts, as is shown in Fig.3.14-Fig.3.16. The figures give the volume changes of various parts of the estuary from 1955 to 1996.

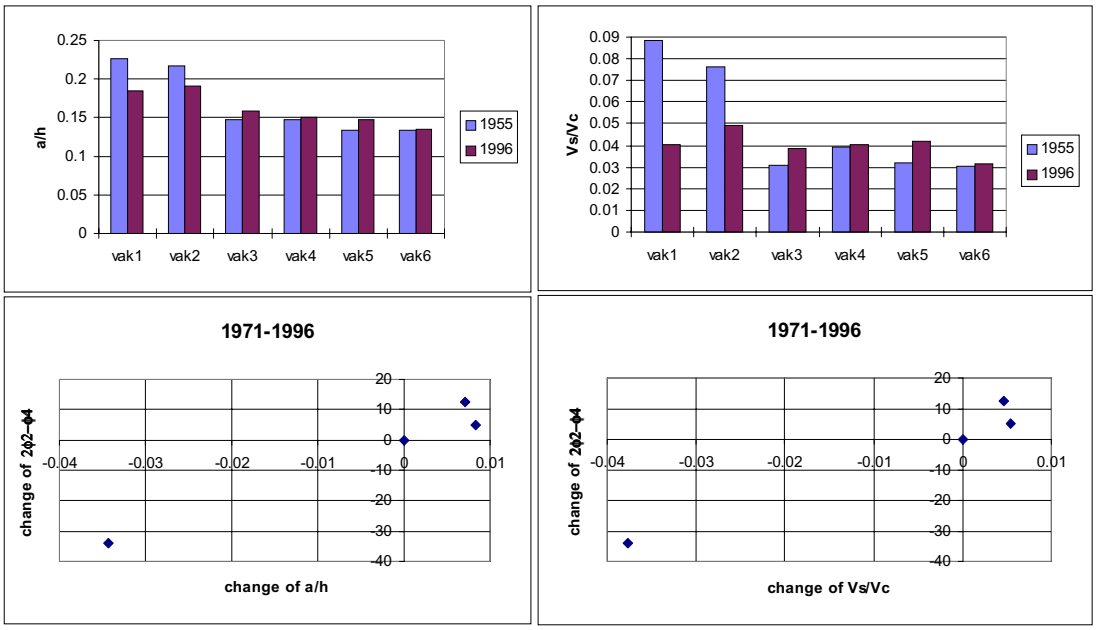

Fig.3.13 Changes of the two morphological parameters as defined by Speer et al (1991) and their relation to the changes of the relative phase difference between M4 and M2

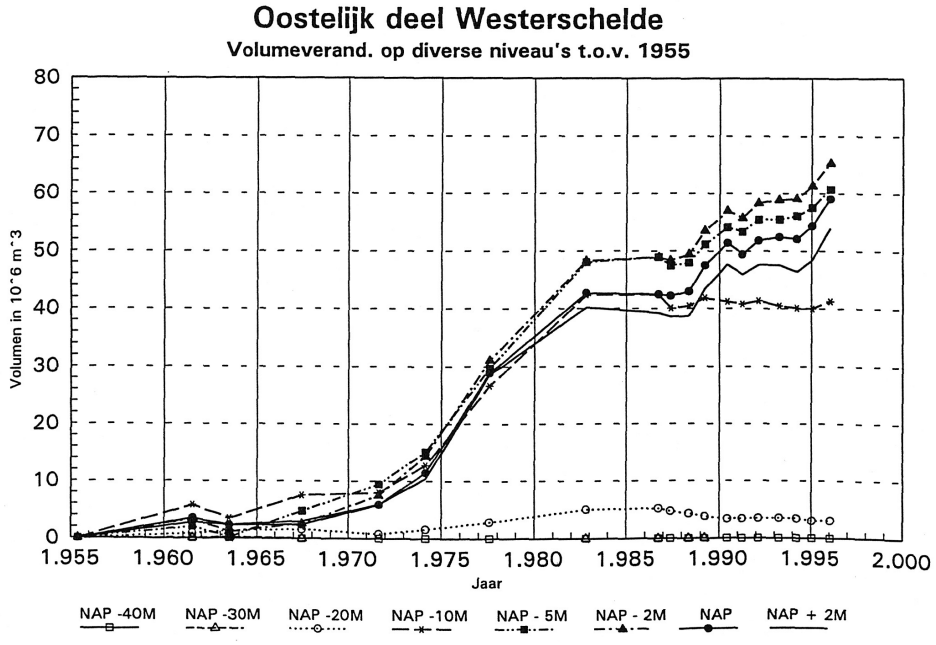

Fig.3.14 Volume changes of eastern part of Western Scheldt (Vak 1 and 2)

Qualitatively the theory of Speer et al (1991), although based on totally different cases, is perfectly applicable to explain the changes of the asymmetry of vertical tide in the Western Scheldt, caused by the quarter-diurnal tide.

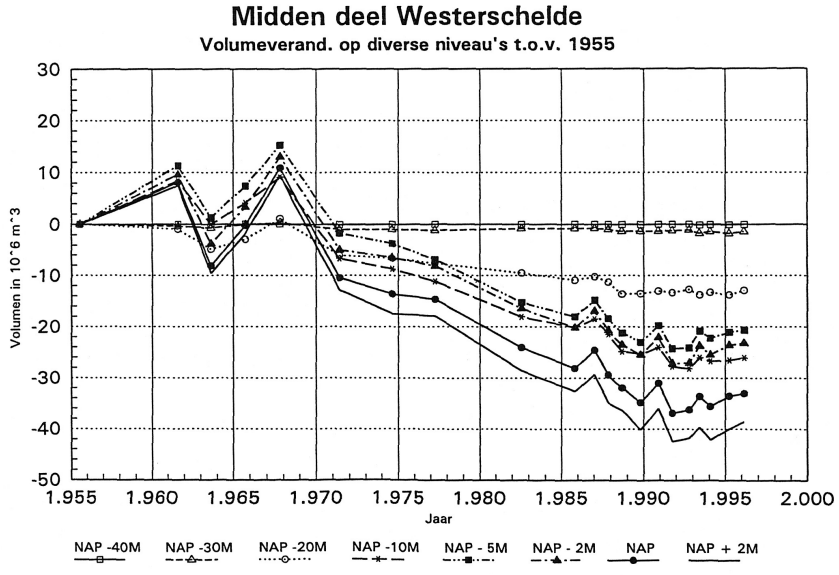

Fig.3.15 Volume changes of the middle part (Vak 3)

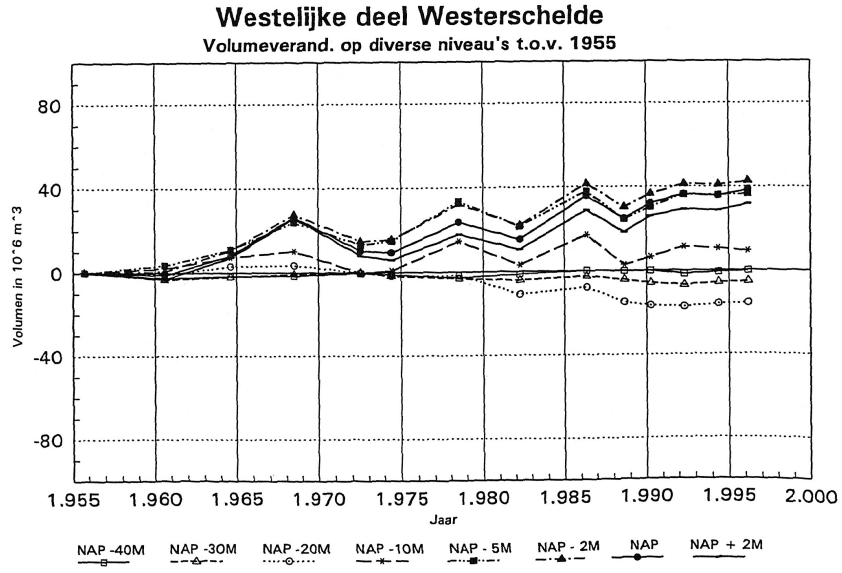

Fig.3.16 Volume changes in the western part (Vak 4, 5 and 6)

3.5.3 Other indicating parameters

Other alternatives

Instead of the two parameters (a/h and V_s/V_c) defined by Speer et al. (1991) the application of other alternative parameters can be considered:

- **Other parameters found in literature.** As described in Chapter 2, there are also other parameters suggested in the literature. An example is the one suggested by Dronkers (1986, section 2.3.3). A similar analysis as described above can be carried out for this parameter. The conclusions will be similar to those drawn for the theory of Speer et al. (1990). This can simply be observed by comparing Fig.3.12 and Fig.2.10.
- **Using independent parameters.** As mentioned in the previous sub-section, the two parameters defined by Speer et al (1991) are not independent of each other. This can be a disadvantage. A possible set of independent parameters containing the same information is e.g. a/h and A_f/A, where the last parameter represents the ratio between the horizontal area of tidal flats and the total area of the corresponding (part of) estuary. It is recommended to consider this set of parameters in the following study
- **The parameters in the fitting equation for the hypsometry.** In combination with the tidal amplitude two dimensionless parameters α and a/d can be defined. The same data as in Fig.3.12 now yield Figure 3.17. It seems that this set parameters has the potential to separate the flood-dominant areas from the ebb-dominant ones. However there is, no theoretical basis for it at this moment (the separator line drawn in the figure is a suggestive one). Furthermore, this set of parameters has its restrictions, since it can only be used in cases where the suggested fitting equation for the hypsometry applies.

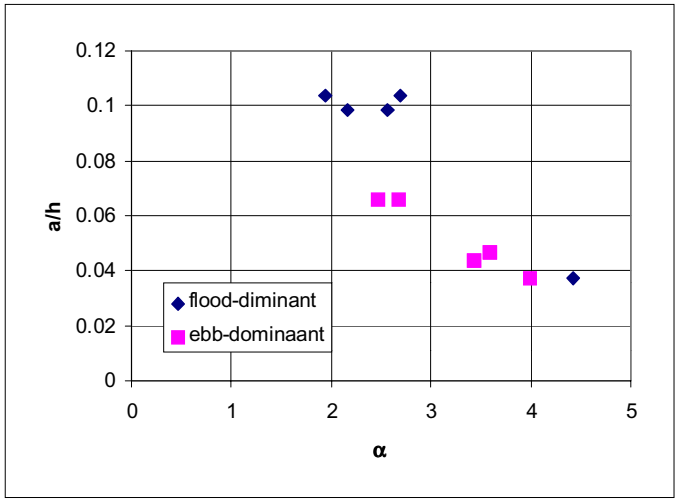

Fig.3.17 Alternative parameters, based on the equation describing the hypsometry in the Western Scheldt, to characterise the ebb/flood dominance of the vertical tide in the estuary.

Additional parameters

The fact that the theories found in the literature are not quantitatively valid for the Western Scheldt indicates that e.g. the parameters defined by Speer et al. (1991) do not form a complete set , in that they cover all relevant aspects of the tidal asymmetry in the estuary. In other words, there must be other parameters which also have influence on the tidal asymmetry and which are (almost) constant for all the cases considered by Speer et al (1991).

As already noted in Chapter 2, all cases considered by Speer et al (1991) concern a fixed length of the estuary, they all concern short and prismatic estuaries, and they are all friction-dominated cases. Making use of the analyses of Li and O'Donnell (1998) on tidal rectification, the following additional parameters are identified:

- The ratio between the length of the estuary and the wave length of the tide.
- The ratio between a length-scale of the morphological variation along the estuary (e.g. the change of width) and the wave length of tide.
- The ratio between the tidal period and the decay time due to friction.

Further research is required to determine the roles of these parameters.

3.5.4 Tidal asymmetry due to sixth-diurnal tide

So far no theory relating the tidal asymmetry caused by the sixth-diurnal tide has been found in the literature. If the same figure as Fig.3.11 for the quarter-diurnal tide is made for the sixth-diurnal tide, one obtains Fig.3.18. As the sixth-diurnal tide plays an important role in the Western Scheldt, it is recommended to carry out research concerning the tidal asymmetry caused by this group of constituents, and its relation with the morphology.

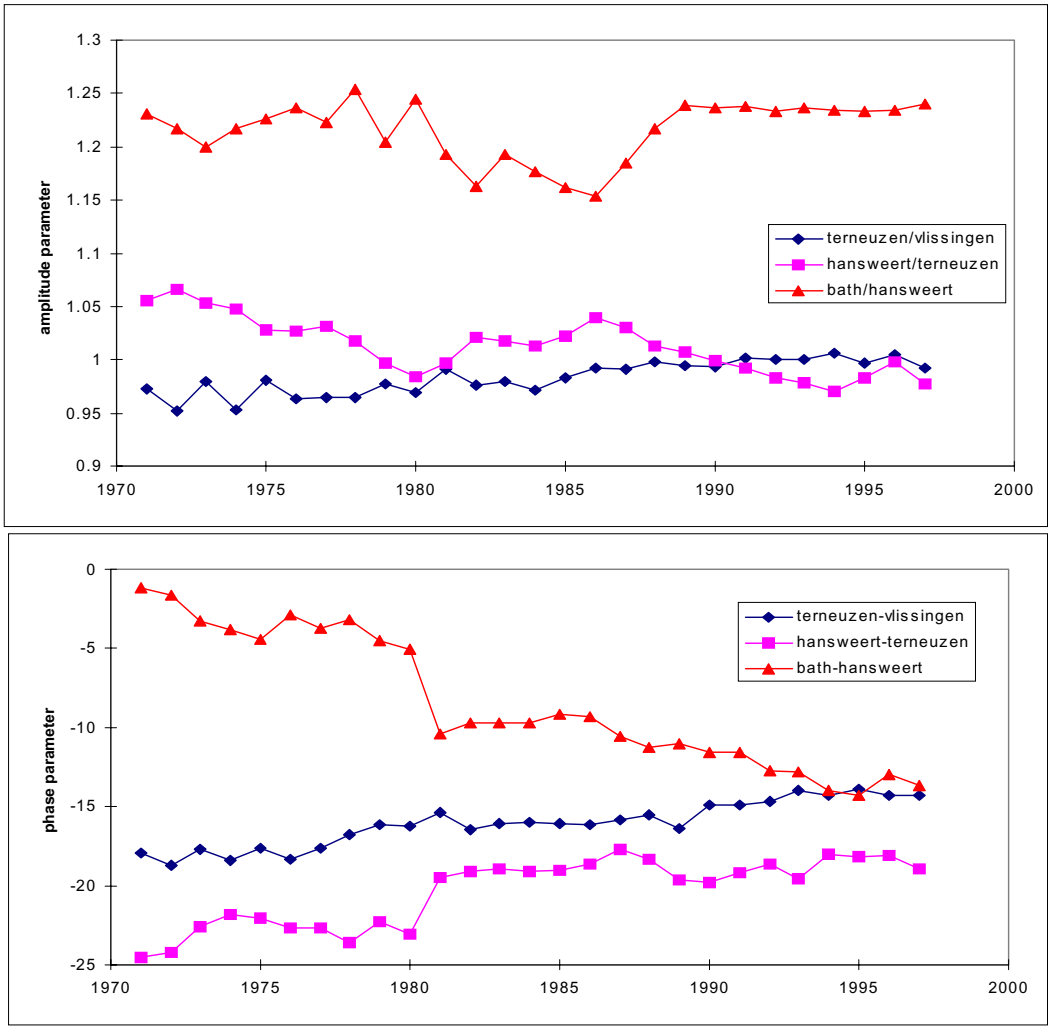

Fig.3.18 Development of the indicating parameters with respect to the downstream station for M6-M2

3.5.5 Concluding discussion

Although the theory found in the literature is not quantitatively applicable to the Western Scheldt, the results presented in the previous sub-sections can readily be used to estimate the changes of the tidal asymmetry due to a certain human interference in the estuary, e.g. a further deepening of the navigation channel. This can be done by determining the two parameters (a/h and V_s/V_c) before and after the interference and plot them in Fig.3.12 and Fig.3.13. The change of the locations of the points before and after the interference gives an indication of the direction in which the tidal asymmetry changes. Based on the available data it is even possible to give a quantitative prediction to a certain extent.

This working method is in fact based on interpolation / extrapolation using the available data. It implies the assumption that the interference will not affect the additional parameters mentioned in 3.5.3 in such a way that the relation between the tidal asymmetry and the two parameters used here will change significantly.

4 Summary, conclusions and recommendations

The objective of the study was to review the theory and concepts on tidal asymmetry and residual sediment transport in estuaries and to asses their applicability to the Western Scheldt estuary. This chapter summarises the principal results and conclusions of the study. Besides it gives some recommendations for further research, to further increase and operationalise the knowledge and understanding of the tidal asymmetry, residual transports and morphologic evolution of the estuary.

The results of the present study were based on the following assumptions and restrictions:

- The estuary is well-mixed: horizontal and vertical density gradients are neglected.
- The estuary is tide-dominated: the influence of a river outflow and meteorological forcings on the water motion and the tidal asymmetry are not considered.
- Most of the theoretical analyses and their applications are based on a 1D approach.
- The period of the M_2 tidal constituent is used as the tidal period.

4.1 Summary and conclusions

Asymmetry refers to the ebb-dominance or flood dominance of the vertical and horizontal tide: the vertical tide is flood-dominant if the duration of falling tide exceeds that of the rising tide. Ebb-dominance occurs in the opposite situation. The horizontal tide (velocity) is considered flood-dominant if it induces a residual sediment transport in landward (flood) direction, whereas it is ebb-dominant in the case of a seaward directed residual sediment transport. The asymmetry of the horizontal tide may be associated with:

- An asymmetry in the magnitude of maximum flow: for instance if maximum flood velocities exceed maximum ebb flow a flood-dominant transport (bed load and suspended load) is likely to occur, as the sediment transport non-linearly increases with the velocity.
- An asymmetry in the duration of slack water: if the duration of slack water before flood (SBF) exceeds the duration of slack water before ebb (SBE) an export (ebb-dominance) of fine suspended sediment is favoured. When the period of slack water before flood lasts shorter the period of slack water before ebb an import of fine suspended sediment is likely to occur.

The astronomical tide and its spatially and temporally varying asymmetry can be described in terms of a number of harmonic components. The amplitude ratio and the phase difference of M_2 and its overtides are often used to characterise the tidal asymmetry.

A theoretical analysis of the individual non-linear terms in the 1D equations of momentum and continuity showed that overtides (M_4 etc.), compound tides (MS4 etc.) and tidal rectification (M_0) are generated by the non-linear interactions of the M_2 tidal component with itself (auto-interaction) and with other fundamental constituents: a time-invariant mean effect (rectification) and the overtide M_4 originate from the auto-interaction of the M_2 via three non-linear terms, viz.: the advective inertia term (B), the bottom friction term (D) and

the discharge gradient term (G). The sixth-diurnal overtide and compound tides (e.g. M_6 , $4MS_6$) are essentially due to the non-linear interaction of M_2 with itself and other fundamental constituents (e.g. S_2) via the bottom friction term (D). This means for instance that in shallow tidal areas characterised by large spatial velocity gradients a generation of M_4 is likely to occur as a result of the auto-interaction of M_2 via the bottom friction term and the advective inertia term.

Residual flows may strongly influence the asymmetry of the horizontal tide. Their generation is very sensitive to spatial variations in bathymetry and horizontal geometry, which makes it a difficult subject to be studied. The residual water motion in the Western Scheldt seems to be dominated by bathymetry-induced residual flows: at many locations in the estuary the total cross-sectionally averaged residual current velocity is the net (small) effect of a relatively large residual flood flow in the flood channel and an ebb-dominated residual flow in the ebb channel. The intensity (magnitude) of residual circulations induced by the ebb and flood channels goes through a neap-spring tidal cycle.

The relationship between the asymmetry of the vertical and the horizontal tide is a non-linear one, because the storage width and cross-sectional area change with the water level (hypsometry effect). This implies that a flood-dominant duration asymmetry of the vertical tide is not necessarily associated with a flood-dominance of the tidal current. The elaboration of this relationship for the Western Scheldt showed that the hypsometric properties of the channel / shoal system tend to reinforce the (quarter diurnal) asymmetry in the flow rates, whereas they tend to weaken the asymmetry in the velocities.

The analysis of some available field observations of the vertical and horizontal tide in the western (seaward) part of the estuary revealed an increase of the tidal asymmetry with the tidal range: during spring tide the asymmetry of the vertical and horizontal tide tends to be stronger than during neap tide. Apparently, the non-linear interactions are stronger during spring tide than during neap tide. The neap-spring-tidal variation finds expression in the generation of the quarter-diurnal and sixth-diurnal compound tides, which may even exceed the magnitude of the overtides M_4 and M_6. The assessment of the implications of this observation for the sediment transports and morphology in the estuary requires new research.

Previous studies on the relationship between the asymmetry of the vertical tide and the overall (estuarine) morphology indicate that the mean channel depth (the parameter a/h) and the inter-tidal area (volume, the parameter V_s/V_c) strongly influence the asymmetry of the vertical tide: shallow estuaries tend to be flood-dominant, whereas deeper estuaries with large inter-tidal areas tend to be ebb-dominant. The theory of Speer et al, (1991) has been evaluated for the Western Scheldt estuary. First, the spatial variations of the quarter-diurnal tidal asymmetry in 1997 and 1971 were compared with the large-scale morphologic characteristics (a/h, V_s/V_c) in 1955/1971 and 1996. This comparison shows that flood-dominance of the vertical tide is indeed associated with larger values of a/h (water depth) and V_s/V_c (inter-tidal area) than in areas where an ebb-dominant tidal asymmetry prevails. Thus, the observations qualitatively agree with the conclusions of Speer et al.(1991). The line that distinguishes ebb-dominance from flood-dominance does not coincide with the results of Speer et al. (1991). This is not surprising since the Western Scheldt significantly differs from the systems studied by Speer et al. (1991).

The evaluation of the theory of Speer et al. (1991) was extended by considering the temporal changes of the tidal asymmetry (of the vertical tide) and the hypsometry. Herein it was hypothesised that the (spatial) change of the tidal asymmetry between two stations, rather than the asymmetry itself, should be related to the morphologic changes (in terms of a/h, V_s/V_c) of the area in between the water level stations. This exercise showed that the theory of Speer et al. (1991) also qualitatively explains the observed changes of the tidal asymmetry and morphology: the deepening of the eastern (landward) part of the estuary was accompanied by a reduction of the flood-dominant asymmetry of the vertical tide. In the western sections of the estuary a small overall shoaling and increase of the inter-tidal area were associated with an increase of the flood-dominance between Vlissingen and Terneuzen and decrease of the ebb-dominance of the between Hansweert and Terneuzen. These results imply that the theory of Speer et al. (1991) may also be applied to assess the impact of human interference on the asymmetry of the vertical tide in a qualitative way. Finally, a few alternative parameters have been identified that may be used to extent the parameterisation of the relationship between tidal asymmetry and estuarine morphology.

4.2 Recommendations

By reviewing the available knowledge in the literature and by analysing the particular situation of the Western Scheldt the results of the present study reveal also the caveats in our knowledge. Further studies are required in order to fill them in.

For the specific situation of the Western Scheldt it is recommended to carry out additional analyses on the following subjects:

- Residual currents. The residual current appears to be one of the important factors influencing the residual sediment transport field in the estuary, but the analysis on this subject in the present study has been restricted.
- Origin of asymmetry of the vertical tide in the Western Scheldt at the process level. This has not been analysed in the present study since this will at least require 1D modelling of the tidal motion in the estuary.
- Mechanisms for sediment transport in the Western Scheldt. The following hypotheses require a verification on the basis of 1-D and 2-D numerical modelling (see also below):
  - The asymmetry (ebb / flood-dominance) of the vertical tide, caused by the generation of overtides, is associated with a similar asymmetry of the horizontal tide (the cross-sectionally-averaged velocity). Thus, a flood-dominant vertical tide is accompanied by maximum flood velocities that exceed the maximum ebb velocities.
  - The direction of the large-scale sediment transport, i.e. integrated over the estuarine cross-section, and the transfer of sediment between estuarine sections depends on the tidal asymmetry induced by the generation of the overtides.
- Effect of sea level rise and 18.6 year tidal cycle.

Most of the knowledge (theories, models, concepts, …) appears applicable to the Western Scheldt in a qualitative, but not directly in a quantitative sense. The following studies should be carried out in order to make the basic knowledge better applicable to the Western Scheldt:

- 1D tidal motion modelling using the hypsometry data / relations of the Western Scheldt and herewith

— determine the separator between ebb- and flood-dominance in the diagram of Speer et al (1991) for the case of the Western Scheldt.
— investigate if an alternative set of indicating parameters will better work for the estuary.
— extend the analysis on the influence of the [2]hypsometry.

- 2DH tidal modelling for the Western Scheldt for further analysis on the residual flow fields in the estuary.

Furthermore, the following analyses are recommended in order to fill in the existing knowledge caveats:

- Analyse the relation between the sixth-diurnal tide and the morphology.
- Analyse the relation between sediment transport and tidal asymmetry for the two-dimensional case: extend the work of Van de Kreeke and Robaczewska (1993) to 2D.
- Analyse the additional parameters influencing the tidal asymmetry.
- Analyse the effect of other factors, e.g. the meteorological forcing , on the sediment transport, and the interaction between these factors and the tidal asymmetry.

2

5 References

Aubrey, D.G. & P.E. Speer (1985) A study of non-linear tidal propagation in shallow inlet/estuarine systems, Part I: observations, Estuarine, Coastal and Shelf Science, Vol. 21, P.185-205.

Aubrey, D.G. (1986), Hydrodynamic controls on sediment transport in well-mixed bays and estuaries, In J. Van de Kreek (ed.) Physics of shallow estuaries and bays, Springer-Verlag, Berlin, p. 245-258.

Aubrey, D.G. & C.T. Friedrichs, (1988), Seasonal climatology of tidal non-linearities in a shallow estuary, In D.G. Aubrey & L. Weishar (eds.), Hydrodynamics and sediment dynamics of tidal inlets, Springer-Verlag, new York, p. 103-124.

Berg, J.H. van den, M.C.J.L. Jeuken & A.J.F. van der Spek (1996), Hydraulic processes affecting the morphology and evolution of the Westerschelde estuary, in: *Estuarine Shores: Evolution, Environments and Human Alternations*, chapter 7, edited by K.F. Nordstrom & C.T. Roman.

Bogaard, L.A. uit den, 1995. Resultaten zandbalans Westerschelde 1955-1993. IMAU rapport R 95-08, Institute for Marine and Atmospheric Research Utrecht

Boon, J.D., 1988, Temporal variation of shallow-water tides in basin-inlet systems, in Aubrey D.G & L. Weishar (eds.), Hydrodynamics and and sediment dynamics of tidal inlets, Springer-Verlag, New York.

Claessens and Meyvis (1994). Het overzicht van de tijwaarnemingen in het Zeeschelde bekken gedurende het decennium 1981-1990. Ministerie van de Vlaamse Gemeenschap. Antwerpse Zeehavendiensten (in Dutch).

Dronkers, J.J., 1964, Tidal computations in rivers and coastal waters, North-Holland Publishing company, Amsterdam.

Dronkers, J., 1986, Tidal asymmetry and estuarine morphology, Netherlands Journal of Sea Research, (20) p.117-131.

Dronkers, J., 1988, Morphodynamics of the Dutch Delta, In Dronkers, J. & M. Scheffers (1998), Physics of Estuaries and Coastal Seas, A.A.BALKEMA, Rotterdam.

Fokkink, R.J., 1998, morphodynamic network simulations of the Western Scheldt, WL | Delft Hydraulics, Report Z0919.

Friedrichs, C.T., Lynch, D.R. & D.G. Aubrey, 1992, Velocity asymmetries in frictionally-dominated tidal embayments: longitudinal and lateral variability, In: Prandle, D.(ed.), Dynamics and exchanges in estuaries and the coastal zone, American Geophysical Union, Washington D.C., P. 277-312.

Friedrichs, C.T. & D.G. Aubrey, (1988), Non-linear tidal distortion in shallow well-mixed estuaries: a synthesis, Estuarine, Coastal and Shelf Science, Vol. 27, P.521-545.

Friedrichs, C.T. & D.G. Aubrey, (1994), Tidal propagation in strongly convergent channels, Journal of geophysical Research, (99) p. 3321-3336.

Friedrichs, C.T. & O.S. Madsen, 1992, Nonlinear diffusion of the tidal signal in frictionally-dominated embayments, Journal of geophysical Research, (97) p. 5637-5650.

Friedrichs, C.T., Aubrey,D.G. & P.E. Speer, (1990), Impacts of relative sea-level rise on evolution of shallow estuaries, In Cheng, R.T. (Ed.), Residual current and long-term transport, Springer-Verlag, New York.

Fry, V.A. & D.G. Aubrey (1990), Tidal velocity asymmetry and bedload transport in shallow embayments, Estuarine, Coastal and Shelf Science, Vol. 30, P.453-473.

Gerritsen, H. & H.F.P. van den Boogaard, 1998. Getijanalyse Westerschelde. Datarapport getijkomponenten, toepassing van Principal Component Analysis. WL | DELFT HYDRAULICS rapport Z2591

Gerritsen, H., Wang, Z.B. & A. van der Weck, 1999, Morfologische interpretatie van de veranderingen in het getij van de Westerschelde, WL | Delft Hydraulics, Report Z2671.

Groen, P., 1967, on the residual transport of suspended matter by an alternating tidal current, Neth. J. Sea Res., 3-4: P.564-574.

Godin, G. (1972). The analysis of tides. Liverpool press.

Huijs, S.E.W., 1995. Geomorfologische ontwikkeling van het intergetijdegebied in de Westerschelde, 1935-1989. IMAU rapport R 95-3, Institute for Marine and Atmospheric Research Utrecht

Jeuken, M.C.J.L. (1996). Hydrodynamics of a bar in a flood channel, the Westerschelde estuary. Proc. Int. Conf. on Coast. Eng. 1996, Orlando. P4491-4504.

Jeuken, M.C.J.L. (1998). De functie en het gedrag van kortsluitgeulen in het westelijk deel van de Westerschelde (eindrapport contract ZL3612). IMAU-report R98-06. Utrecht University.

Jeuken, M.C.J.L. (in prep). Phd-thesis in preparation.

Kerkhoven, J.D.M. van, 1995, Morphological modelling of ebb and flood channel systems in estuaries, Master thesis, Delft University of Technology, Faculty of Civil Engineering.

Kjerfve, B., 1978, Bathymetry as an indicator of net circulation in well mixed estuaries, Limnol. Oceanogr., 23(4), 816-821.

Kreek, J. van de, 1981, Tide-induced residual flow in shallow bays, Journal of Hydraulic research, 19(3), p.231-249.

Kreeke, J. van de & K. Robaczewska, 1993. Tide induced residual transport of coarse sediment; application to the Ems estuary. Netherlands Journal of Sea Research 31 (3): 209-220, Netherlands Institute for Sea Research.

Le Provost, C. and M. Fornerino (1985). Tidal spectroscopy of the English Channel with a numerical model. J. of Phys. Oceanography, 15: 1009-1031.

Li, C. & J. O'Donnell, 1997, Tidally drivven residual circulation in shallow estuaries with lateral depth variation, Journal of Geophyisical Research, 102(C13), p. 27915-27929.

Louters, T., 1998, Verkenning effecten versnelde zeespiegelstijging op dynamiek Westerschelde getijsysteem, Literatuurstudie, DHV, rapport IS-NW980254.

Male, C. van der, 1993, Euleriaanse reststromen op de Westerschelde berekend met DETWES., Werkdocument GWWS 93.839x. Rijkswaterstaat, RIKZ, Middelburg.

Mol, et. al. (1997)

Mol, G., 1999. Analyse harmonische componenten in de Westerschelde; periode 1971-1997. Werkdocument RIKZ/AB-99.805x, Rijksinstituut voor Kust en Zee/RIKZ

Parker, B.B., 1991, The relative importance of the various nonlinear mechanisms in a wide range of tidal interactions (review), in Parker B.B. (ed.) Tidal hydrodynamics, J. Wiley & Sons, New York.

Pieters, T. & C. Verspuy, 1997. Getijananalyse Schelde-estuarium. Invloed plaatselijke veranderingen bergende oppervlakte op getijvoortplanting, een analyse met Trecos-Westerschelde 1997. Rapport BGW - 97.6, Bureau Getijdewateren.

Proudman (1923).

Proudman (1955)

Provost, Ch.L., 1991, Generation of overtides and compound tides (review), in in Parker B.B. (ed.) Tidal hydrodynamics, J. Wiley & Sons, New York.

Ridderinkhof, H., 1988a, tidal and residual flows in the Western Dutch Wadden Sea, I: Numerical model results, Netherlands Journal of Sea Research, 22(1), P.1-21.

Ridderinkhof, H., 1988b, tidal and residual flows in the Western Dutch Wadden Sea, II: An analytical model to study the constant flow between connected tidal basins, Netherlands Journal of Sea Research, 22(3), P.185-198.

Ridderinkhof, H., 1989, tidal and residual flows in the Western Dutch Wadden Sea, III: Vorticity balances, Netherlands Journal of Sea Research, 23(1), P.9-26.

Slikke, A. van der, 1997. Grootschalige zandbalans van de Westerscheldemonding (1969-1993). Een inventarisatie van de dieptegegevens (1800-1996). IMAU rapport R 97-18, Instituut voor Marien en Atmosferisch Onderzoek Utrecht.

Speer, P., Aubrey, D.C. and C.T. Friedrichs, 1991, Nonlinear hydrodynamics of shallow tidal inlet/bay systems, in Parker B.B. (ed.) Tidal hydrodynamics, J. Wiley & Sons, New York.

Speer, P.E. & D.G. Aubrey (1985) A study of non-linear tidal propagation in shallow inlet/estuarine systems, Part II: Theory, Estuarine, Coastal and Shelf Science, Vol. 21, P.207-224.

Spek, A.F. (1994). Large-scale evolution of Holocene tidal basins in the Netherlands. Phd-thesis. Utrecht University.

Tee, T.K., 1976, Tide-induced residual current, 2 2D nonlinear numerical tidal model, Journal of Marine Research, 34, P.603-628.

Veen, J. van, 1950, Eb en vloedschaar systemen in de Nederlandse getijwateren, Tijdschrift KNAG, 2e series, deel 67, p.303-325.

Vroon, J.H., C. Storm & J. Coosen (1997) *Westerschelde, stram of struis*, evaluation report of the OOSTWEST project concerning the Western Scheldt, National Institute of Coastal and Marine Management (in Dutch).

Zimmerman, J.T.F., 1978, Topographic generation of residual circulation by oscillatory (tidal) currents, Geophys. Astrophys. Fluid Dynamics, vol. 11, p.35-47.

Zimmerman, J.T.F., 1980, Vorticity transfer by tidal currents over an irregular topography, Journal of Marine Research, 38(4), p.601-630.

Zimmerman, J.T.F., 1981, Dynamics, diffusion and geomorphological significance of tidal residual eddies, Nature, Vol.290, p.549-555.

A Periodicity and period of tide

In the strict mathematical sense a function of time t is periodic with the period T if for many value of t

$$f(t+T) = f(t) \tag{A.1}$$

As a simple example the following function

$$f(t) = \cos(\omega t) \tag{A.2}$$

is periodic with the period

$$T = \frac{2\pi}{\omega} \tag{A.3}$$

In this sense the tidal variation of e.g. water level is not periodic. This can be demonstrated by considering the periodicity of the following function:

$$f(t) = \cos(\omega_1 t) + \cos(\omega_2 t) \tag{A.4}$$

This function will only be periodic if the ratio between the two frequencies is a rational number:

$$\frac{\omega_1}{\omega_2} = \frac{n_1}{n_2} \tag{A.5}$$

The period will then be

$$T = n_1 \frac{2\pi}{\omega_1} = n_2 \frac{2\pi}{\omega_2} \tag{A.6}$$

The sum of more cosines functions will only be periodic if the ratios between all the frequencies are rational numbers. For three cosines this is case if

$$\frac{\omega_1}{\omega_2} = \frac{n_1}{n_2} \text{ and } \frac{\omega_2}{\omega_3} = \frac{n_3}{n_4} \tag{A.7}$$

The period in this case is

$$T = m \frac{2\pi}{\omega_2} \tag{A.8}$$

where m is the common multiple of n_2 and n_3.

In the case of tidal variation many cosines are involved and the frequencies of them are determined by the motion of the celestial bodies. It is almost impossible that the all the ratios between these frequencies are rational numbers since there are much more irrational numbers than rational numbers. Even if it were periodic the period would be very large.
Although the tide is not periodic we do talk about tidal period, by which we usually mean the period of the dominating (often M_2) tidal constituent. A more strict definition may be the time interval between two high waters or between two flood slacks. If such a strict definition is used the tidal period is no more a constant but varies from tide to tide. This can be demonstrated by considering a tide consisting of two constituents (e.g. M_2 and S_2).

$$\zeta(t) = a_{M2}\cos(\omega t) + a_{S2}\cos(\omega t + \Delta\omega t) \tag{A.9}$$

The high and low waters are determined by

$$\frac{\partial \zeta}{\partial t} = -\omega a_{M2}\sin(\omega t) - a_{S2}(\omega + \Delta\omega)\sin(\omega t + \Delta\omega t) = 0 \tag{A.10}$$

or

$$\tan(\omega t) = \frac{-\dfrac{a_{S2}(\omega + \Delta\omega)}{a_{m2}\omega}\sin(\Delta\omega t)}{1 + \dfrac{a_{S2}(\omega + \Delta\omega)}{a_{m2}\omega}\cos(\Delta\omega t)} \tag{A.11}$$

The solution of this equation is shown in the following figure demonstrating that the time interval between high and low waters are varying in time.

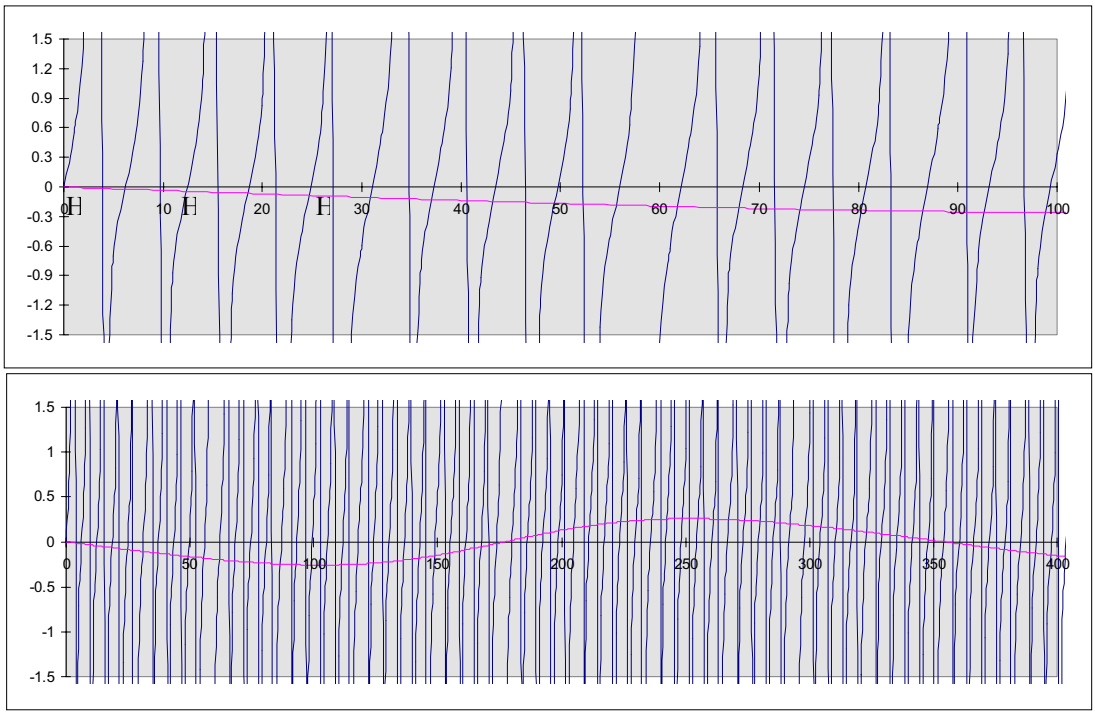

Fig.A.1 The high and low waters occur at the cross points between the tangent function with the frequency of the M_2 tide and the periodic function (right hand side of A.11) with the beat frequency. The first three high waters are indicated at the upper figure which is a zoom in of the lower figure.

B 1-D equations for the tidal motion in a channel with variable width

The cross-sectionally integrated, 1-D equations of motion for well-mixed, channelised flow in a tidal embayment with intertidal flats may be expressed as (e.g. Speer and Aubrey, 1985) :

$$\underbrace{\frac{\partial u}{\partial t}}_{(A)}+\underbrace{u\frac{\partial u}{\partial x}}_{(B)}+\underbrace{g\frac{\partial \zeta}{\partial x}}_{(C)}+\underbrace{c_f\frac{u|u|}{h_0+\zeta}}_{(D)}=0$$

$$\underbrace{b\frac{\partial \zeta}{\partial t}}_{(E)}+\underbrace{\frac{\partial}{\partial x}\{b_c u(h_0+\zeta)\}}_{(F)}=0$$

in which:

t	=	time,
x	=	distance to channel entrance,
$u(x,t)$	=	cross-sectionally averaged flow velocity,
$\zeta(x,t)$	=	water surface elevation w.r.t. mean sea level,
h_0	=	water depth below mean sea level,
g	=	acceleration due to gravity, and
c_f	=	bed friction factor
b	=	total embayment width (including flats)
b_c	=	the width of the channel

(A) the local inertia term,
(B) the advective inertia term,
(C) the slope term,
(D) the bottom friction term.

The terms in the equation of continuity, are:

(G) the storage term, and
(H) the discharge gradient term.